

Vapor Pressure Osmometry Studies of Osmolyte–Protein Interactions: Implications for the Action of Osmoprotectants in Vivo and for the Interpretation of “Osmotic Stress” Experiments in Vitro[†]

E. S. Courtenay,[‡] M. W. Capp,[§] C. F. Anderson,[§] and M. T. Record Jr.,^{*,§,||}

Departments of Bacteriology, Chemistry, and Biochemistry, University of Wisconsin—Madison, 433 Babcock Drive, Madison Wisconsin 53706

Received December 16, 1999; Revised Manuscript Received February 1, 2000

ABSTRACT: To interpret or to predict the responses of biopolymer processes in vivo and in vitro to changes in solute concentration and to coupled changes in water activity (osmotic stress), a quantitative understanding of the thermodynamic consequences of interactions of solutes and water with biopolymer surfaces is required. To this end, we report isoosmolal preferential interaction coefficients (Γ_{μ_1}) determined by vapor pressure osmometry (VPO) over a wide range of concentrations for interactions between native bovine serum albumin (BSA) and six small solutes. These include *Escherichia coli* cytoplasmic osmolytes [potassium glutamate (K^+Glu^-), trehalose], *E. coli* osmoprotectants (proline, glycine betaine), and also glycerol and trimethylamine *N*-oxide (TMAO). For all six solutes, Γ_{μ_1} and the corresponding dialysis preferential interaction coefficient Γ_{μ_1,μ_3} (both calculated from the VPO data) are negative; Γ_{μ_1,μ_3} is proportional to bulk solute molality (m_3^{bulk}) at least up to 1 *m* (molal). Negative values of Γ_{μ_1,μ_3} indicate preferential exclusion of these solutes from a BSA solution at dialysis equilibrium and correspond to local concentrations of these solutes in the vicinity of BSA which are lower than their bulk concentrations. Of the solutes investigated, betaine is the most excluded ($\Gamma_{\mu_1,\mu_3}/m_3^{bulk} = -49 \pm 1 \text{ m}^{-1}$); glycerol is the least excluded ($\Gamma_{\mu_1,\mu_3}/m_3^{bulk} = -10 \pm 1 \text{ m}^{-1}$). Between these extremes, the magnitude of $\Gamma_{\mu_1,\mu_3}/m_3^{bulk}$ decreases in the order glycine betaine \gg proline $>$ TMAO $>$ trehalose $\approx K^+Glu^- >$ glycerol. The order of exclusion of *E. coli* osmolytes from BSA surface correlates with their effectiveness as osmoprotectants, which increase the growth rate of *E. coli* at high external osmolality. For the most excluded solute (betaine), Γ_{μ_1,μ_3} provides a minimum estimate of the hydration of native BSA of approximately $2.8 \times 10^3 \text{ H}_2\text{O}/\text{BSA}$, which corresponds to slightly less than a monolayer (estimated to be $\sim 3.2 \times 10^3 \text{ H}_2\text{O}$). Consequently, of the solutes investigated here, only betaine might be suitable for use in osmotic stress experiments in vitro as a direct probe to quantify changes in hydration of protein surface in biopolymer processes. More generally, however, our results and analysis lead to the proposal that any of these solutes can be used to quantify changes in water-accessible surface area (ASA) in biopolymer processes once preferential interactions of the solute with biopolymer surface are properly taken into account.

Sugars, amino acids and their derivatives, and other small solutes are transported or synthesized to high [~ 0.1 – 1 m (molal)] intracellular concentrations in both prokaryotic and eukaryotic cells in response to the stress of a high osmolality environment (1–17). After an osmotic upshift, intracellular accumulation of these solutes (called osmolytes or osmoprotectants) allows the cell to increase its volume by increasing the amount of cellular water and thereby to resume growth (osmolytes) or to increase growth rate (osmoprotectants) (18, 19 and references therein). In vitro, these solutes typically stabilize the native state of globular proteins and favor the formation of protein assemblies (1, 11, 12, 19–24). Increases in the concentration of such solutes generally

drive protein processes in the direction that reduces the amount of water accessible surface area (ASA).¹ Solutes that function as osmoprotectants in vivo have been shown (or are proposed to be) excluded from biopolymer surface in vitro (10–12, 19, 21). Preferential exclusion of osmolytes from biopolymer surface has been proposed to be the physical basis of their evolutionary selection (25 and references therein).

To obtain a quantitative thermodynamic and molecular understanding of the effects of osmolytes and osmoprotectants on processes involving native proteins in vitro and in vivo, we have determined the extent of interaction of six such solutes with a native protein in vitro. This study tests two hypotheses: (i) that the differences in interactions of *E. coli* cytoplasmic solutes (osmolytes) with protein surface

[†] This research was supported by NIH Grant GM47022. E.S.C. was supported in part by a National Research Service Award 5T32GM08349 from NIGMS.

* To whom correspondence should be addressed.

[‡] Department of Bacteriology.

[§] Department of Chemistry.

^{||} Department of Biochemistry.

¹ Abbreviations: ASA, water-accessible surface area; BSA, bovine serum albumin; *E. coli*, *Escherichia coli*; K^+Glu^- , potassium glutamate; Osm, osmolality; PNAI, protein-nucleic acid interactions; TMAO, trimethylamine *N*-oxide; VPO, vapor pressure osmometry.

correlate with differences in their effectiveness as osmoprotectants, and (ii) that the effect of changes in small solute concentration on processes involving native proteins, though not simply determined by changes in protein hydration, can nevertheless be used to quantify changes in the ASA of the proteins. Evidence supporting both these hypotheses regarding small solutes and osmoprotectants is developed in this paper. Background relevant to these hypotheses is presented in the following sections.

Small Solutes as Cellular Osmolytes and Osmoprotectants in Vivo. Small solutes commonly used as osmolytes or osmoprotectants by *E. coli* and other organisms include trehalose [used by bacteria, fungi, and actinomycetes (2, 3, 9, 13, 18)]; proline [used by many bacteria, marine invertebrates, some plants, and some mammalian cells (1, 2, 4–13, 16, 18)]; glycine betaine [used by many bacteria, halophilic archaeobacteria, marine invertebrates, and plants (1, 2, 7–18)]; glycerol [used by some yeasts, plants, and many insects (1, 13)]; and trimethylamine *N*-oxide [TMAO, used by many marine invertebrates and some vertebrates (1)]. These osmolytes are called “compatible” solutes (1, 12, 21) because they do not destabilize (and indeed in many cases stabilize) the native state of proteins and protein assemblies. The osmolyte potassium glutamate [K^+Glu^- ; used by *E. coli*, some other eubacteria, and some mammalian cells (2, 5, 6, 8, 9, 13, 16, 18)] is unusual in that protein–nucleic acid interactions (PNAI) typically are destabilized by an increase in salt concentration (19, 20 and references therein). Global cellular mechanisms have been proposed to explain the insensitivity of *E. coli* PNAI to changes in cytoplasmic K^+ concentration in vivo. These mechanisms involve changes in amounts of other solutes and of water that compensate for the perturbing effects of K^+ concentration. They include changes in putrescine concentration at low osmolality (26), and changes in macromolecular crowding at high osmolality (9). By analogy, increases in the cytoplasmic concentration of “compatible” uncharged osmolytes should require a compensating reduction in macromolecular crowding and/or changes in other cellular variables to avoid large perturbations (i.e., overstabilization) of cellular processes such as protein binding and assembly.

E. coli adapts to and grows over more than a 100-fold range of external osmolalities [~ 0.02 –3 Osm (18 and references therein)] by varying the amounts of cytoplasmic solutes and water over wide ranges. Above 0.28 Osm in minimal growth medium (in the presence or absence of osmoprotectants), Cayley et al. (9, 10) found that growth rate appears fundamentally correlated with the amount of free cytoplasmic water (i.e., water that is not “bound” as biopolymer water of hydration). After initially losing water upon a shift from low to high external osmolality, *E. coli* accumulates cytoplasmic osmolytes by transport [potassium (K^+); proline or glycine betaine if available] and biosynthesis [trehalose, glutamate (Glu^-)] in order to increase the amount of free cytoplasmic water and increase growth rate (9, 10, 18). In 1 Osm minimal growth medium, Cayley et al. (10) found that the *E. coli* cytoplasm contains similar total amounts of osmolytes both in the presence and absence of added osmoprotectants, but dramatically different amounts of free water. In the absence of osmoprotectants, where the cytoplasmic osmolytes are K^+ , organic anions (including glutamate) and trehalose, *E. coli* exhibits a modest growth

rate (~ 0.5 generations/h). Uptake of proline or glycine betaine, when available, replaces some or all of these osmolytes and allows both an increase in free cytoplasmic water and in growth rate (both increase ~ 1.3 -fold with proline and ~ 1.7 -fold with betaine). The amount of cytoplasmic water, the K^+ concentration, and the growth rate achieved at 1 Osm in the presence of glycine betaine are comparable to the values characteristic of *E. coli* growing at ~ 0.4 Osm in the same minimal medium without betaine.

Thermodynamic Description of Solute–Biopolymer Interactions. Effects of polyols and other “compatible” solutes on the equilibrium concentration quotient (K_{obs}) and corresponding standard free-energy change ($\Delta G_{obs}^\circ = -RT \ln K_{obs}$) of biopolymer processes² are often interpreted entirely in terms of changes in the amount of water of hydration that accompany the conversion of biopolymer reactants to products (22). However, the dependence of ΔG_{obs}° or K_{obs} for a biopolymer process on the concentration of any small solute is determined fundamentally by differences in preferential interaction coefficients characterizing the interactions of the small solute with products and reactants in the process and cannot be interpreted only in terms of the changes in biopolymer hydration that accompany the process (20, 21, 27, 28). In the Discussion, we develop our previous proposal (29) that only a solute which is “completely excluded” from water of biopolymer hydration can be used directly to probe changes in water of hydration. Our results with BSA and literature data (21 and references therein, 29) on various proteins argue strongly that no solute yet characterized (or used in osmotic stress studies on protein processes), except possibly glycine betaine, meets this criterion. Consequently, the interpretation of effects of changes in solute concentration on ΔG_{obs}° or K_{obs} of biopolymer processes requires a quantitative characterization of the interactions of solutes with biopolymer surface, relative to interactions with water.

Interactions between a small solute and a biopolymer relative to their interactions with water are quantified using preferential interaction coefficients. Three different but closely related preferential interaction coefficients are used in this paper (defined and explained in the next section). Developments in the thermodynamic theory of multicomponent systems (20, 21, 24, 30–33) and in experimental methods to determine preferential interaction coefficients (21, 29, 30, 34) have increased our understanding of solute–biopolymer interactions and of solute effects on biopolymer processes. Timasheff and co-workers have carried out an extensive series of experimental studies characterizing interactions of selected electrolyte and nonelectrolyte solutes with various globular proteins by dialysis in conjunction with densimetry (reviewed in ref 21). Eisenberg and co-workers experimentally characterized the interactions of salts and nonelectrolyte solutes with proteins and DNA using dialysis/densimetry, analytical ultracentrifugation, and light-, X-ray-, or neutron-scattering experiments (30, 34). Our laboratory recently introduced vapor pressure osmometry (VPO) as a sensitive method of characterizing solute–protein interactions and their osmotic consequences (29). However, despite the large body of work describing the interactions of both uncharged and charged solutes with proteins and nucleic acids, few systematic or comparative studies have been

² R is the gas constant (cal/mol K) and T is the Kelvin temperature.

performed to characterize preferential interactions of small solutes with one biopolymer as a function of small solute concentration. In addition, no predictive capability of the effects of these solutes on homologous biopolymers (differing in the amount but not the general physical characteristics of their surface area) and on their processes has been achieved.

Information in the form of preferential interaction coefficients (Γ) describing interactions (relative to water) between small solutes and biopolymer surfaces allows the quantitative prediction or interpretation of effects of the nature and concentration of the small solute on the thermodynamics of biopolymer processes. Generally, preferential interaction coefficients for a three-component solution describe how the molalities of the two solute components are linked when three thermodynamic functions are maintained constant (30). Effects of an uncharged solute at activity a_3 on $\Delta G_{\text{obs}}^\circ$ or K_{obs} for a process involving uncharged (or weakly charged) biopolymers are predicted or interpreted in terms of preferential interaction coefficients Γ_{μ_3} (defined in the following section) (20, 21, 32):

$$-(1/RT)(\partial \Delta G_{\text{obs}}^\circ / \partial \ln a_3) = (\partial \ln K_{\text{obs}} / \partial \ln a_3) = \Delta \Gamma_{\mu_3} \quad (1)$$

$\Delta \Gamma_{\mu_3}$ is the stoichiometrically weighted difference in solute–biopolymer preferential interaction coefficients where each Γ_{μ_3} characterizes the interactions of the small solute with a product or reactant of the biopolymer process.³ Effects of a 1:1 electrolyte solute at mean ionic activity a_{\pm} on $\Delta G_{\text{obs}}^\circ$ or K_{obs} for a process involving charged or uncharged biopolymers are predicted or interpreted in terms of stoichiometric differences in preferential interaction coefficients of the individual ions (Γ_+ , Γ_-) using the equation (20, 28, 33)

$$-(1/RT)(\partial \Delta G_{\text{obs}}^\circ / \partial \ln a_{\pm}) = (\partial \ln K_{\text{obs}} / \partial \ln a_{\pm}) = \Delta \Gamma_+ + \Delta \Gamma_- \quad (2)$$

a result which is readily generalized to other salt ion valences.

Relationship of Osmolality to Preferential Interactions of a Small Solute and Water with a Biopolymer. In this paper, we advance the development of vapor pressure osmometry [VPO (29)] as an accurate method of determining the preferential interaction coefficients that quantify the interactions of the small solutes glycerol, K^+Glu^- , trehalose, proline, betaine, and TMAO with bovine serum albumin (BSA), a very soluble protein with a relatively large surface-to-volume ratio (35). The vapor pressure osmometer measures the activity of water⁴ in a solution at a given temperature and pressure. Determining solution osmolality as a function of small solute molality in the presence and absence of protein allows comparison of the three- and two-component solutions at the same water activity.⁵ This information is used to determine the isoosmolal preferential interaction coefficient designated Γ_{μ_1} , defined by the partial derivative and approximated by the quotient of differences:

$$\Gamma_{\mu_1} \equiv (\partial m_3 / \partial m_2)_{T,P,\mu_1} \cong (m_3 - m_3^\Delta) / m_2 \quad (3)$$

where m_2 and m_3 are the molalities of protein and small solute in the protein solution and m_3^Δ is the small solute molality in the two-component solution at the same water activity as the three-component solution.

In addition to the isoosmolal Γ_{μ_1} , two preferential interaction coefficients defined with the constraint of constant solute chemical potential μ_3 (Γ_{μ_3} , Γ_{μ_1,μ_3}) are evaluated in this work. The preferential interaction coefficient Γ_{μ_3} is defined by the partial derivative with the constraints of constant T , P , and μ_3 and approximated by the quotient of differences:

$$\Gamma_{\mu_3} \equiv (\partial m_3 / \partial m_2)_{T,P,\mu_3} \cong (m_3 - m_3^*) / m_2 \quad (4)$$

where m_3^* is the small solute molality in the two-component solution at the same temperature, pressure, and small solute chemical potential as in the three-component solution. Preferential interaction coefficients of this type are used to analyze the dependence of the thermodynamics of a biopolymer process on small solute concentration (cf. eqs 1 and 2) (20, 31–33). Direct experimental determinations of Γ_{μ_3} are feasible only in special cases such as for a solution containing component 2 in equilibrium with solid-phase component 3 at constant temperature and pressure.

The preferential interaction coefficient Γ_{μ_1,μ_3} (generally measurable by dialysis) is defined by the partial derivative with the constraints of constant T , μ_1 , and μ_3 and approximated by the quotient of differences:

$$\Gamma_{\mu_1,\mu_3} \equiv (\partial m_3 / \partial m_2)_{T,\mu_1,\mu_3} \cong (m_3 - m_3') / m_2 \quad (5)$$

where m_3' is the molality of small solute in a two-component solution in dialysis equilibrium with the three-component solution [the biopolymer (component 2) cannot diffuse across the membrane]. Approximation of any of the derivatives in eqs 3–5 by the corresponding quotient of concentration differences between the two solutions (\pm protein) is accurate under conditions where the quotient is independent of protein molality m_2 .

The preferential interaction coefficient Γ_{μ_1,μ_3} defined in eq 5 can be determined directly from a dialysis experiment in which a small solute is equilibrated between a biopolymer solution and water and is interpreted most simply in the context of the local–bulk domain model (20, 28). The terms “accumulation” and “exclusion” of the solute are defined experimentally by the relative molal concentrations of the small solute in the two solutions in dialysis equilibrium. Accumulation refers to the situation where Γ_{μ_1,μ_3} is positive and the concentration of solute in the biopolymer solution exceeds its concentration in the two-component solution. Exclusion refers to the situation where Γ_{μ_1,μ_3} is negative and the concentration of the small solute in the two-component solution is higher than in the biopolymer solution. If the concentrations of small solute are the same on both sides of the membrane, Γ_{μ_1,μ_3} is zero. Accumulation in the biopolymer solution implies local accumulation of the solute in the vicinity of the biopolymer relative to its bulk concentration; likewise, exclusion from the biopolymer solution implies local exclusion of the solute from the vicinity of the biopolymer. This relationship between local solute–solvent

³ In eq 1, the partial derivatives are taken at constant temperature and pressure and at sufficiently low concentration of all stoichiometric participants in the process so that changes in their activity coefficients are due entirely to their interactions with the small solute (33).

⁴ $\text{Osm} \equiv -55.5 \ln a_1$

⁵ This is equivalent to a comparison at constant chemical potential of water μ_1 when temperature and pressure are also constant, as they were during each set of VPO measurements analyzed here.

partitioning and Γ_{μ_1, μ_3} is the basis of the local/bulk domain interpretation of Γ_{μ_1, μ_3} (20, 28).

Analysis of Osmometric Data to Obtain Γ_{μ_3} and Γ_{μ_1, μ_3} . A rigorous thermodynamic relationship between Γ_{μ_3} (eq 4) and Γ_{μ_1} (eq 3) is obtained from the three-component solution Gibbs–Duhem relationship at constant temperature and pressure (see Appendix 1 and ref 36):

$$\Gamma_{\mu_3} = (\Gamma_{\mu_1} + Q)/[(m_2 \Gamma_{\mu_1}/m_3) + 1] \quad (6)$$

where Q is defined as the quotient:

$$Q \equiv (\partial \mu_2 / \partial \ln m_2)_{m_3} / (\partial \mu_3 / \partial \ln m_3)_{m_2} \quad (7)$$

The partial derivatives in eq 7 are taken at constant temperature, pressure, and the indicated solute molality.

Neither derivative in eq 7 is experimentally accessible by direct measurement. However, Γ_{μ_3} in eq 6 can be evaluated from VPO data by introducing one (or both) of two independent approximations (36). One approximation equates the derivative $(\partial \mu_2 / \partial \ln m_2)_{m_3}$ for a three-component solution to its value in the corresponding two-component solution where $m_3 = 0$, which can be evaluated exactly using VPO and the Gibbs–Duhem equation for the two-component solution:

$$(\partial \mu_2 / \partial \ln m_2)_{m_3} \cong -m_1 (\partial \mu_1 / \partial m_2)_{m_3=0} = RT(\partial \text{Osm} / \partial m_2)_{m_3=0} \quad (8)$$

where $m_1 = 55.5$ mol/kg. From eqs 3, 4, 8, and the three-component Gibbs–Duhem equation, the following expression for Γ_{μ_3} is obtained (cf. Appendix 1 and also ref 36):

$$\Gamma_{\mu_3} \cong (\Gamma_{\mu_1} + R_1)/[1 + (m_2/m_3)(\Gamma_{\mu_1} + R_1)] \quad (9)$$

where

$$R_1 \equiv (\partial \text{Osm} / \partial m_2)_{m_3=0} / (\partial \text{Osm} / \partial m_3)_{m_2} \quad (10)$$

Both derivatives in R_1 are measurable by VPO.

An alternative independent approximation equates the derivative $(\partial \mu_3 / \partial \ln m_3)_{m_2}$ for a three-component solution to its value in the corresponding two-component solution where $m_2 = 0$. In this case, use of the two-component Gibbs–Duhem equation allows the denominator of Q to be related to the experimentally accessible derivative of the osmolality of the two-component solution ($m_2 = 0$) with respect to solute concentration:

$$(\partial \mu_3 / \partial \ln m_3)_{m_2} \cong -m_1 (\partial \mu_1 / \partial m_3)_{m_2=0} = RT(\partial \text{Osm} / \partial m_3)_{m_2=0} \quad (11)$$

In this approximation, eq 6 reduces to eq 12, in which Γ_{μ_1} has been eliminated (36):

$$\Gamma_{\mu_3} \cong (m_3/m_2)(1 - R_2) \quad (12)$$

where R_2 is defined as the following ratio of derivatives, both of which are measurable by VPO:

$$R_2 \equiv (\partial \text{Osm} / \partial m_3)_{m_2} / (\partial \text{Osm} / \partial m_3)_{m_2=0} \quad (13)$$

The preferential interaction coefficient Γ_{μ_1, μ_3} (eq 5) that characterizes solute–biopolymer interactions under conditions of dialysis equilibrium is calculated from values of Γ_{μ_1} and Γ_{μ_3} using the exact relationship (derived in ref 36):

$$\Gamma_{\mu_1, \mu_3} = \frac{\bar{V}_3 \Gamma_{\mu_1} \left(\frac{m_2}{m_1} \Gamma_{\mu_3} - \frac{m_3}{m_1} \right) - \bar{V}_1 \Gamma_{\mu_3}}{\bar{V}_3 \left(\frac{m_2}{m_1} \Gamma_{\mu_3} - \frac{m_3}{m_1} \right) - \bar{V}_1} \quad (14)$$

where \bar{V}_3 and \bar{V}_1 are the partial molar volumes of the small solute and of water. Γ_{μ_1, μ_3} is the preferential interaction coefficient which is most directly interpretable in terms of local–bulk partitioning of the solute, using the rigorous derivation of the local–bulk domain model (20, 28).

The three different coefficients discussed here, Γ_{μ_1} , Γ_{μ_3} , and Γ_{μ_1, μ_3} , are all referred to as preferential interaction coefficients (30) but each describes a different thermodynamic linkage between the two solute molalities (m_2 and m_3). The values and physical interpretations of each of these coefficients are not generally equivalent but (as shown above in eq 14) can all be related to one another. The necessity of considering each of these preferential interaction coefficients is due to a combination of differences in their experimental accessibility, in the extent to which each can be compared with existing literature data, and in their thermodynamic and molecular significance. [We discuss these differences in greater detail elsewhere (36)].

EXPERIMENTAL PROCEDURES

Solutes. Glycine betaine monohydrate (>99% pure, FW 135.2), D(+) trehalose dihydrate (FW 378.3), monopotassium salt glutamic acid (>99% pure, FW 185.2), and L-proline (SigmaUltra >99% pure, FW 115.1) were obtained from Sigma (St. Louis, MO). Spectrophotometric grade (>99.5% pure) glycerol (FW 92.09) was obtained from Aldrich (Milwaukee, WI). Rather than attempt to obtain water-free glycerol, the amount of water contained in our glycerol stock was determined by comparison of its density (measured on an Anton Paar DMA 5000 density meter) with the published value for the density of pure glycerol at 25 °C (37). Trimethylamine *N*-oxide dihydrate (TMAO) (>99% pure, FW 111.14) was obtained from Fluka (Milwaukee, WI). All of the compounds listed above were used without further purification.

Bovine Serum Albumin (BSA). Two different preparations of BSA (66 411 g mol^{−1}) were obtained from Sigma (St. Louis, MO) to investigate by VPO: fraction V, Sigma no. A6918, and Sigma no. A0281, minimum 99% pure, essentially fatty acid-free, globulin-free lyophilized powder. In both cases, 20 g samples of BSA were dissolved in 100 mL of 10 mM Na₂HPO₄, 100 mM NaCl, 2 mM EDTA (Na₂) at pH 7.5 and dialyzed in two 30 cm lengths of standard dialysis tubing (Spectrum, MMCO 12–14 kDa) against 4 L of this solution overnight. Each BSA solution was then dialyzed, first against 4 L of 10 mM NaCl for 6 h, then against 4 L of 2.5 mM NaCl for 3 h, and subsequently against three 4 L batches of deionized water, each for at least 9 h. The extensive dialysis removes all low molecular mass contaminants (including fatty acids and other weakly bound

Table 1: Solution pH for Two- and Three-component Systems

solute	two-component solution		three-component solution		
	m_3 (m) ^a	pH	BSA, $m_2 \times 10^3$ (m)	solute, m_3 (m)	pH
glycerol	4.22	3.86	3.32	4.22	6.76
trehalose	1.91	5.46	3.81	1.91	6.73
proline	1.99	6.26	3.80	1.99	6.82
betaine	3.73	6.59	3.25	3.73	7.18
K ⁺ Glu [−]	1.18	7.20	3.40	1.18	7.13
TMAO	1.87	8.97	2.45	1.87	7.50
BSA			3.00	0	6.83

^a m , molal.

molecules) from the BSA (35). The dialyzed protein was then lyophilized for 3 days. The dry protein was quickly transferred to a Nalgene jar, sealed with Parafilm, and stored at -20°C .

Several comparisons were made between the two BSA samples after they were prepared as described above. Osmometric measurements with glycerol, performed on both samples, were identical within experimental uncertainty. Extinction coefficients, determined experimentally immediately after extensive lyophilization from the absorbance in Tris (0.01 M) EDTA (0.001 M) buffer, were the same within uncertainty for both samples ($6.50 \pm 0.14 \text{ cm}^{-1}$) as the value calculated from the amino acid composition of BSA: $\epsilon_{280\text{nm}}^{1\%} = 6.49 \pm 0.13 \text{ cm}^{-1}$ (38). This value (6.50 cm^{-1}) was used to determine the concentrations of all BSA solutions. In the absence of small solutes, the two BSA solutions showed small but significant differences in the BSA concentration dependence of solution osmolality; A0281 BSA deviated more significantly from ideal solution behavior. The pH (at 25°C) was determined for solutions of each small solute with and without BSA using a Fisher Accumet AR10 pH meter with a 6 mm probe on 1 mL samples. The results are presented in Table 1.

Coomassie blue and silver staining of denaturing PAGE (7.5% acrylamide) gels run using a 20-fold range of protein concentrations showed that the A6918 BSA contained fewer impurities (both high and low molecular mass) than the A0281 BSA. When gels were coomassie stained, protein impurities in the A6918 BSA were only clearly visible by eye when the gel was overloaded for BSA ($\sim 0.7 \text{ mg/mL}$ BSA loaded), while impurities were clearly visible in the A0281 BSA at $\sim 0.3 \text{ mg/mL}$ BSA loaded. This demonstrated that our preparation of A6918 BSA was at least as pure as the A0281 BSA ($>99\%$ pure as provided by Sigma). The A6918 BSA preparation was used for all of the experiments reported here. To check for the presence of oligomers of BSA in our preparation, native PAGE gels were run at several different protein concentrations. In lanes at relatively low BSA concentration (0.23 mg/mL BSA, where the monomer band is not overloaded), both a dimer band and a weaker tetramer band are visible ($\sim 6:1$ ratio), together accounting for 10–15% of the total protein. To test whether aggregation increases with increasing BSA concentration, native gels were run over about a 200-fold protein concentration range (up to 39 mg/mL BSA loaded). In these gels (extremely overloaded for monomer BSA), the amount of monomer of course could not be quantified but the ratio of dimer to tetramer (6:1) was the same as in the nonoverloaded

native gel, indicating that the percentage of aggregates does not increase with increasing BSA concentration. These results are in agreement with sedimentation equilibrium experiments where no concentration dependence of the amounts of BSA oligomers (11% of total protein) was observed (39), and where the monomer fraction was purified from the oligomer fraction by size-exclusion chromatography and subsequently remained 100% monomeric (within experimental uncertainty) upon reequilibration (40). For the quantities of protein necessary for the experiments reported here, chromatographic purification of the BSA would have been impractical. The presence of 10–15% small oligomers in our BSA solutions (maximum estimate) could not reduce the total solvent-accessible surface area of BSA in the solution by more than $\sim 5\%$, an amount that is within the uncertainty of our surface area calculation (see below). The results of the native gel analysis and our experimental finding that the measured thermodynamic parameters are independent of protein concentration (see Results) provide no evidence of concentration-dependent aggregation.

Preparation of Solutions for VPO Determinations of Preferential Interaction Coefficients. In the approach introduced here to analyze VPO measurements, Γ_{μ_1} is calculated as the difference in small solute molality between a solution containing the protein [three-component (+BSA)] and a reference [two-component (−BSA)] solution compared at the same water activity, temperature, and pressure. The quality of the results is determined primarily by the accuracy and reproducibility with which the molalities of both protein and small solute can be determined. To simplify the analysis of the VPO data, all of the experimental solutions would be made up on the molal concentration scale so that the molality of the protein could be fixed while the molality of the small solute is varied. Reasons for choosing molality as the basis for the thermodynamic expressions used here in analyzing VPO data are discussed in the Appendix in ref 36. However, fixing the protein molality would require gravimetric addition of completely dry protein and small solute to a known mass of water for each three-component solution. We found that freshly lyophilized BSA accumulates $\sim 10\%$ water⁶ during storage at -20°C in a Parafilm sealed Nalgene jar. Consequently, we prepared all protein solutions in deionized water, measured the protein concentration (mg/mL) of a serially diluted aliquot spectrophotometrically ($\sim 2\%$ error due to uncertainty in the extinction coefficient), and then obtained a series of solutions with the same protein molarity and various concentrations of the small solute by combining accurately known volumes of protein solution ($21 \pm 0.1 \mu\text{L}$) and of a solution of the small solute ($14 \pm 0.1 \mu\text{L}$). Molal concentrations of the protein and solute were then calculated using partial molar volumes of the solute and protein measured by densimetry (as described below).

In the course of this work, we found that gravimetric methods of preparing the small solute solutions reduced the experimental error relative to the volumetric methods reported previously (29). The effect was significant for the less excluded solutes. All experiments with TMAO, K⁺Glu[−], all but one with glycerol, and half of those with trehalose

⁶ Percentage water by weight was determined by comparing the extinction coefficient determined directly after lyophilization with that determined after 1 week of storage.

Table 2: Summary of Solute Partial Molar Volumes and Dependences of Solution Osmolality on Solute Molality for Two- and Three-Component Solutions

solute (small solute)	two-component solutions			three-component solutions	
	partial molar volume (L/mol) $\times 10^2$	$(\partial \text{Osm}/\partial m_3)_{m_2=0}$	range (m); no. of solutions ^a	$(\partial \text{Osm}/\partial m_3)_{[2]}^b$	range (m); no. of solutions ^a
glycerol	7.09 ± 0.01	$1 + (0.0128 \pm 0.0002)m_3$	$m_3 \leq 3.5$; $n = 130$	1.047 ± 0.003	$m_3 \leq 3.1$, $m_2 = (3.1-3.8) \times 10^{-3}$; $n = 31$
K ⁺ Glu ⁻	$9.08 \pm 0.05 + (0.3 \pm 0.1)m_3$	1.76 ± 0.01	$m_3 \leq 0.864$; $n = 36$	1.84 ± 0.02	$m_3 \leq 0.97$, $m_2 = (2.3-2.5) \times 10^{-3}$; $n = 26$
trehalose	20.97 ± 0.03	$1 + (0.18 \pm 0.02)m_3$	$m_3 \leq 0.600$; $n = 107$	$1.09 \pm 0.04 + (0.16 \pm 0.16)m_3$	$m_3 \leq 0.65$, $m_2 = (2.9-3.3) \times 10^{-3}$; $n = 49$
TMAO	7.24 ± 0.04	$1 + (0.36 \pm 0.01)m_3$	$m_3 \leq 1.25$; $n = 50$	$1.07 \pm 0.02 + (0.42 \pm 0.05)m_3$	$m_3 \leq 1.5$, $m_2 = (3.1-3.4) \times 10^{-3}$; $n = 35$
proline	$8.32 \pm 0.04 + (0.07 \pm 0.03)m_3$	$1 + (0.096 \pm 0.007)m_3$	$m_3 \leq 1.87$; $n = 90$	$1.12 \pm 0.05 + (0.09 \pm 0.05)m_3$	$m_3 \leq 2.2$, $m_2 = (2.9-3.4) \times 10^{-3}$; $n = 47$
betaine	9.82 ± 0.03	$1 + (0.40 \pm 0.01)m_3$	$m_3 \leq 0.869$; $n = 142$	$1.20 \pm 0.09 + (0.56 \pm 0.15)m_3$	$m_3 \leq 1.05$, $m_2 = (3.8-4.2) \times 10^{-3}$; $n = 45$
solute (BSA)	partial molar volume (L/mol)	$(\partial \text{Osm}/\partial m_2)_{m_3=0}$	range (m); no. of solutions ^a		
BSA	49.17 ± 0.05	$5.1 \pm 0.9 + [(1.8 \pm 0.4) \times 10^3]m_2$	$m_2 \leq 6.9 \times 10^{-3}$; $n = 11$		

^a n is the number of independently prepared solutions. Three aliquots of each were measured in the osmometer. ^b The subscript [2] represents constant BSA molarity.

were obtained using solutions made up gravimetrically. A known mass of small solute (of known water content, if not completely anhydrous) and a known mass of deionized water was added to a series of weighed microcentrifuge tubes to produce a final volume of approximately 1 mL. Each tube in such a series contains increasing amounts of small solute. All masses were determined on a Mettler analytical balance with an error of ± 0.1 mg. All other experiments reported here (with proline and betaine, as well as half of the trehalose experiments, and one glycerol experiment) were made up volumetrically by a previous procedure (29). Micropipets were gravimetrically calibrated (and tested three times for volume reproducibility) using deionized water before pipetting each volume. After a protein stock and 12 small solute solutions of increasing molality were made as described above, 14 μL of each small solute solution (either the gravimetrically prepared solutions or the volumetric serial dilutions) were combined with 21 μL of the BSA stock or of deionized water to give 35 μL total. We have routinely achieved single-volume pipetting precision of 0.1% or better (standard deviation). Three 10 μL aliquots of each solution were read in the osmometer.

Partial specific (or molar) volumes of each solute are required to determine the molal concentrations of small solute and protein present in our solutions. The partial molar volume of water is assumed to be the same as for pure water at 25 °C ($\bar{V}_1^\circ = 0.01807$ L/mol); solute partial specific volumes were determined from densimetry experiments on BSA and small solute two-component solutions (see Table 2 for experimentally determined partial molar volumes). The density of each solution was measured with a vibrating-tube density meter (DMA 5000, Anton Paar), accurate to at least five decimal places. From these data, the effect of each solute's concentration on its partial specific volume in

deionized water was investigated. For all of the solutes except proline and K⁺Glu⁻, the partial specific volume was found to be constant over the entire concentration range studied. The partial molar volume of proline increases by 1.5% as its concentration increases from 0.13 to 1.87 m . The partial molar volume of K⁺Glu⁻ increases by 2.9% as its concentration increases from 0 to 0.9 m . Both concentration dependences (reported in Table 2) were accounted for in our calculations of proline and K⁺Glu⁻ molalities.

For a two-component system, the conversion from molar to molal concentration scales is given by

$$m_i = \frac{[i]}{m_1 \bar{V}_1 - [i] \bar{V}_i} \quad (15)$$

where m_i and m_1 are the molalities of solute (small solute or BSA, as appropriate) and of water, $[i]$ is the molar concentration of solute; \bar{V}_i and \bar{V}_1 are the partial molar volume of the small solute (or BSA) and of water. For the biopolymer and the small solute in a three-component solution, the corresponding expression for conversion from molarity to molality is

$$m_i = \frac{[i]}{m_1 \bar{V}_1 - [i] \bar{V}_i - [j] \bar{V}_j} \quad (16)$$

where i is the solute of interest (molal concentration m_i) and j is the other solute.

VPO Determinations of Osmolality as a Function of Solute Concentration. The osmolalities of three aliquots of each solution (both with and without BSA for each small solute concentration) were measured in Wescor 5500 or VAPRO 5520 vapor pressure osmometers (Logan, UT). For each solute (except K⁺Glu⁻), data was obtained using both

osmometers; K^+Glu^- solutions were measured in the Wescor 5500 instrument. The data sets for each small solute included at least 36 individually made solutions; three measurements on each solution were made in the osmometer. For a given solute, data representing the dependence of osmolality on solute molality for the two-component solutions were fitted by a quadratic equation [$Osm = m_i(a + bm_i)$; for uncharged small solutes the fitting parameter a was fixed at 1 and b was floated; for BSA and K^+Glu^- , a and b were both floated]. Data were weighted by the standard deviation of sets of three osmometric measurements obtained on independent aliquots of the same solution using a nonlinear fitting program [NONLIN (41)]. Using a cubic function did not improve any fittings of the data; for BSA and all small solutes, the fitted value of the cubic coefficient was zero within error.

For evaluation of R_1 and R_2 (eqs 10 and 13), the dependence of solution osmolality on small solute molality at constant BSA molarity is converted to the corresponding dependence at constant BSA molality using the following relationship (derived in the second section of Appendix 1):

$$\left(\frac{\partial Osm}{\partial m_3}\right)_{m_2} = \frac{\left(\frac{\partial Osm}{\partial m_3}\right)_{[2]}}{1 - \left(\frac{[2]\bar{V}_3\Gamma_{\mu_1}}{1 - [2]\bar{V}_2}\right)} \quad (17)$$

Despite different operating temperatures [37 °C for the 5500; ambient temperature (24–25 °C) for the VAPRO 5520], the two osmometers yielded identical osmolality data for all systems above 40 mOsm. Below 40 mOsm, the Wescor 5500 osmometer cannot be calibrated to give a reading for deionized water of 0 mOsm and, therefore, gives systematically high readings. For this reason, all data points below 40 mOsm were measured in the VAPRO 5520 osmometer. Before each experiment, the thermocouple of the instrument was cleaned using an ammonium hydroxide solution (Wescor cleaning solution) and deionized water. The thermocouple was then dried completely, allowed to equilibrate thermally in the instrument, and calibrated at least twice in immediate succession using standard solutions supplied by Wescor (100, 290, and 1000 mOsm). The criteria used for having properly cleaned and calibrated the thermocouple were reproducible readings of the osmolal standards and a reading of zero for deionized water in the VAPRO 5520 osmometer. After each set of measurements at a particular small solute concentration, readings for deionized water and the standard solutions were checked. The instrument was recalibrated if the deionized water reading had drifted above 2 mOsm or if readings for any of the standards deviated by more than 2 mOsm. If the deionized water reading increased 5 mOsm after any set of measurements and remained high after recalibration, the thermocouple was recleaned and calibrated. Frequent thermocouple cleaning was necessary for maintaining proper instrument calibration throughout the experiments. We found that it was difficult to maintain proper calibration of the VAPRO 5520 when the relative humidity exceeded 42%. All data reported here were obtained below 42% relative humidity.

Determination of Water-Accessible Surface Area (ASA) of BSA. The ASA of BSA was estimated from the ASA of

the homologous human serum albumin (HSA; 85% identical in primary sequence to BSA) ($\sim 2.8 \times 10^4 \text{ \AA}^2$) calculated from the crystal structure (42) using a previously described algorithm (43). No electron density was distinguishable for residues 1–27 and 608–609 in the crystal structure. A conservative estimate of the surface area contribution of each of these residues in solution is obtained by assuming that their fractional exposure to water is the same as that of the average for that type of residue in HSA [alanine (two residues, each 29 \AA^2); arginine (three residues, each 55 \AA^2); aspartate, 78 \AA^2 ; glycine, 10 \AA^2 ; histidine, 51 \AA^2 ; isoleucine, 18 \AA^2 ; leucine (six residues, each 20 \AA^2); lysine (two residues, each 97 \AA^2); methionine, 13 \AA^2 ; phenylalanine (three residues, each 15 \AA^2); serine (four residues, each 30 \AA^2); threonine (two residues, each 58 \AA^2); tryptophan, 53 \AA^2 ; tyrosine, 19 \AA^2 ; valine (two residues, each 20 \AA^2). From these values, we predict $1 \times 10^3 \text{ \AA}^2$ for the residues not resolved in the HSA crystal structure and thereby obtain the total ASA of $\sim 2.9 \times 10^4 \text{ \AA}^2$ for BSA used in calculations in this paper. (The alternative assumption of maximal exposure of these residues would yield a maximum ASA contribution of $\sim 3 \times 10^3 \text{ \AA}^2$ and a total ASA of $3.1 \times 10^4 \text{ \AA}^2$).

RESULTS

Comparison of Osmolalities of Solutions of E. coli Osmolytes in the Presence and Absence of a Protein at Physiological Concentrations Demonstrates the Thermodynamic Basis of Osmoprotection. To characterize the interactions between a representative protein (BSA) and six small solutes of physiological and biochemical significance, we have measured the dependence of osmolality on small solute concentration in the presence and absence of BSA. For the four *E. coli* osmolytes (K^+Glu^- , trehalose, proline, and glycine betaine), VPO measurements of solution osmolality as a function of small solute concentration are shown in panels A–D of Figure 1 for representative fixed BSA concentrations. Panels E and F of Figure 1 show corresponding VPO studies for TMAO and glycerol. In all cases, the three-component solution osmolality at zero small solute molality is the osmotic contribution of the indicated molar concentration of the BSA. For all six solutes, the (vertical) difference in osmolality between the three-component (+BSA) solution and the two-component (–BSA) solution increases with increasing small solute molality. In other words, for all six solutes at any specified molal concentration, the presence of BSA increases the osmolality over that of the –BSA control by an amount (i) which always exceeds the osmolality of the corresponding BSA solution in the absence of small solute and (ii) which increases with increasing molal concentration of the small solute.

Figure 1 demonstrates qualitatively that the effects of these small solutes on solution osmolality differ from one another. However, because K^+Glu^- is a dissociated electrolyte and the other solutes are uncharged, the osmolality scales differ in Figure 1. In addition, the BSA concentrations are not the same for the six solutes investigated. To illustrate more directly the differences in the small solute concentration dependences of osmolality and the nonadditivity of the osmotic contributions of the protein and each of these six solutes, Figure 2 shows the increase in osmolality as a result of the presence of $3 \times 10^{-3} \text{ m}$ BSA (calculated from the

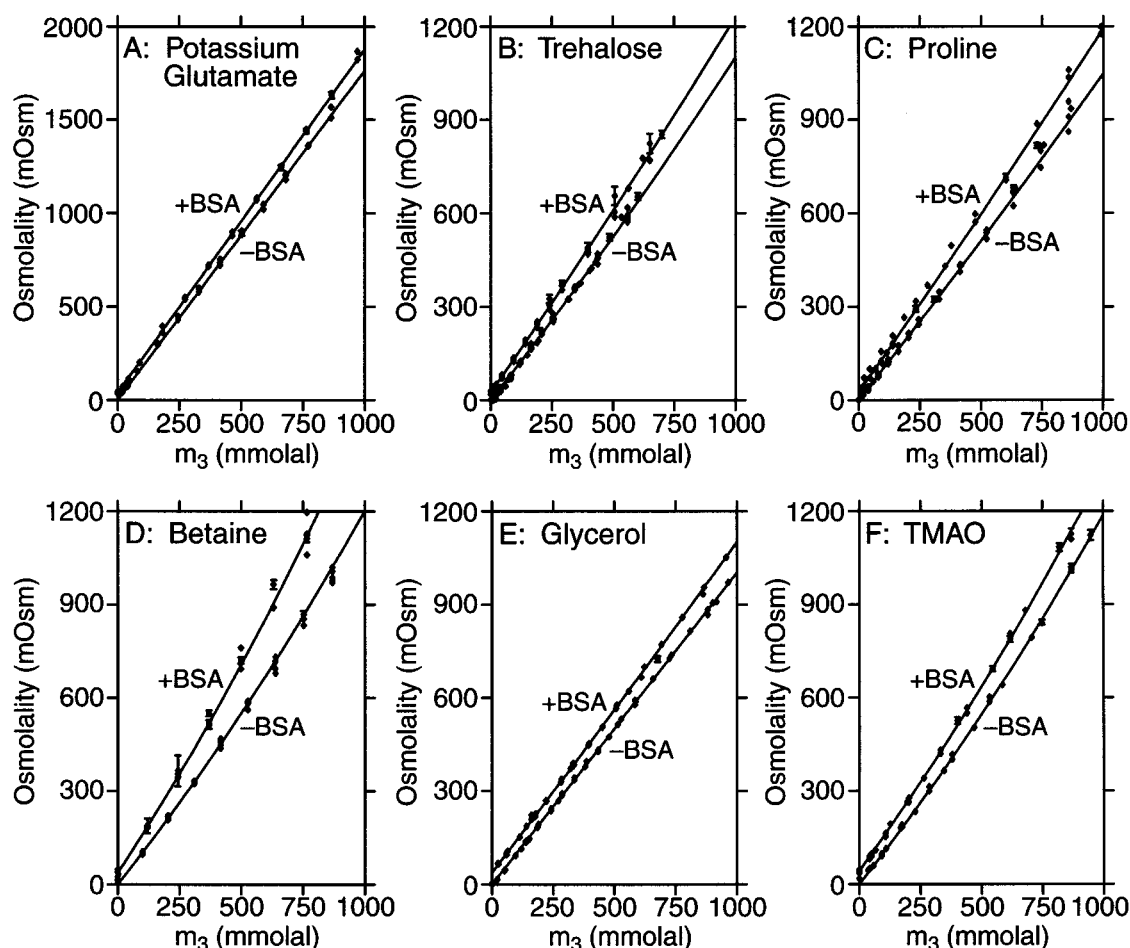


FIGURE 1: Solution osmolality as a function of small solute molality (millimoles per liter) in three-component (water-BSA-solute) and two-component (water-solute) solutions. Panels A–F show raw data for solutions of $\text{K}^+\text{Glu}^- \pm 2.07$ mM BSA, trehalose ± 2.55 mM BSA, proline ± 2.55 mM BSA, glycine betaine ± 3.51 mM BSA, glycerol ± 2.70 mM BSA, and TMAO ± 2.69 mM BSA, respectively. Error bars represent the standard deviation of triplicate osmometric measurements for each solution; solid curves represent the least-squares fit to the data (see Experimental Procedures).

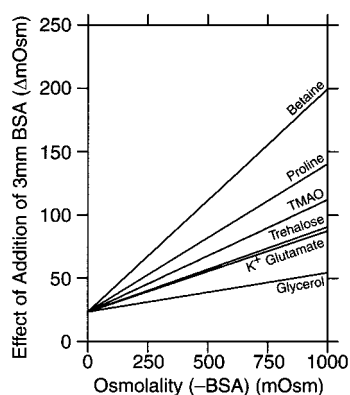


FIGURE 2: Change in solution osmolality upon the addition of 3×10^{-3} m BSA as a function of the osmolality of the two-component solution without BSA. Osmolality of the two-component solutions is directly calculated from the fittings to the osmolality versus small solute molality data (cf. lower curves in Figure 1); the osmolality of the three-component solutions at a constant BSA molality was calculated from Γ_{μ_3} (eq 12) for each solute.

analysis of data of Figure 1 and other VPO experiments) as a function of the osmolality of a two-component solution of the small solute (–BSA). This BSA concentration (approximately 200 mg/mL in the absence of added small solute) is in the physiological range of total protein concentration in *E. coli* (18).

Figure 2 shows the significant differences between the osmotic effects of these solutes in a protein solution as well as the extreme nonadditivity of the osmolality of these solutions. When compared at the same osmolality of the small solute solution (–BSA), the largest osmolality increase upon the addition of 3 mM BSA is obtained for glycine betaine, and the rank order of solutes in this regard is glycine betaine > proline > TMAO > trehalose, K^+Glu^- > glycerol. The increase in osmolality of a 1 Osm betaine–water solution upon addition of 3 mM BSA (0.024 Osm in the absence of betaine) is 20% (1–1.2 Osm), more than eight times the osmolality increase predicted by an additivity relationship; for glycerol, the effect is 3%, or about twice the increase predicted by additivity. The molecular basis of the dramatic effect of the addition of BSA on the osmolality of a glycine betaine solution is that both BSA and glycine betaine prefer to be hydrated rather than to interact with one another. Indeed, betaine–BSA preferential interaction coefficients, obtained from these VPO measurements and analyzed using the local–bulk domain model of the small solute partitioning (28), indicate that on average no significant population of betaine molecules is present in the surface layer of water of hydration of BSA (see below). Adding a given amount of protein to a solution containing a solute that is locally excluded from the protein surface raises the osmolality of the solution far more than would be observed if the

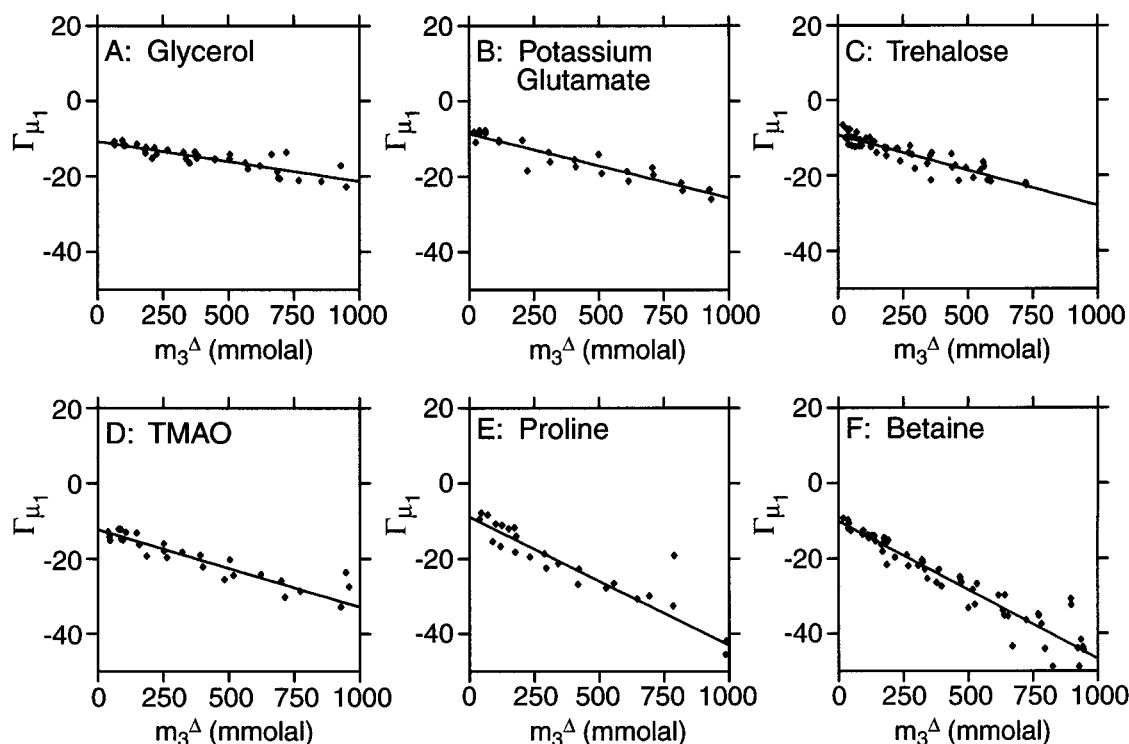


FIGURE 3: Γ_{μ_1} as a function of small solute molality in the two-component solution ($-$ BSA) at the same temperature, pressure, and chemical potential of water as the three-component solution ($+$ BSA). Panels A–F show data for glycerol (at 1.83, 2.7, 2.86, 2.96, and 3.1 mM BSA), K^+Glu^- (at 2.07 mM BSA), trehalose (2.55, 2.85, and 3.04 mM BSA), TMAO (2.69 and 3.06 mM BSA), proline (2.55 and 3.51 mM BSA), and glycine betaine (1.79, 2.56, 2.72, and 3.19 mM BSA), respectively. Solid lines represent the nonlinear least-squares fit to the data. The uncertainty in individual data points [based on the standard deviation of triplicate osmometric measurements for each solution (cf. Figure 1)] is smaller than the symbols shown.

osmotic contributions of the solute and the protein were simply additive. The other solutes investigated here, for which the addition of BSA yields smaller osmolality increases (cf. Figure 2), are less excluded from BSA; interactions of these solutes with BSA are therefore somewhat more favorable than for glycine betaine; although in all cases, the bulk solute concentration is predicted to exceed its local concentration near BSA.

Determination of Isoosmolal Preferential Interaction Coefficients (Γ_{μ_1}) Characterizing the Thermodynamic Consequences of Solute–Protein Interactions. Comparative analysis of the small solute concentration dependences of the osmolality of three-component solutions and of the corresponding two-component ($-$ BSA) solutions for several BSA concentrations allows us to calculate the preferential interaction coefficient at constant water chemical potential, Γ_{μ_1} , as a function of small solute molality for each solute–protein interaction (cf. eq 3). In the absence of BSA, the five nonelectrolyte solutes exhibit quadratic dependences of solution osmolality on small solute molality in which the constant term is zero and the coefficient of the first-order term is unity. For the electrolyte potassium glutamate, solution osmolality is proportional to K^+Glu^- molality with a proportionality constant of 1.76 (see column 2, Table 2). For an isoosmolal analysis of these data to obtain Γ_{μ_1} (eq 3), interpolation of the fitted data (represented by the lower solid curve in each panel of Figure 1) describing solution osmolality as a function of small solute molality ($-$ BSA) is used to obtain the small solute molality, (m_3^Δ), in the two-component solution at the same osmolality as the three-component solution.

The isoosmolal preferential interaction coefficient Γ_{μ_1} is calculated by eq 3 as the difference between the small solute molalities in the three- and two-component solutions at the same osmolality divided by the protein molality in each three-component solution. For the six solutes and the range of BSA concentrations investigated, Figure 3 shows all experimental data for Γ_{μ_1} as a function of the small solute molality (m_3^Δ) in the two-component solution. Figure 3 shows that Γ_{μ_1} is a linear function of small solute molality (m_3^Δ) and that calculated values of Γ_{μ_1} (from eq 3) determined at different BSA concentrations fall on a common line, indicating no BSA concentration dependence of Γ_{μ_1} and hence validating the isoosmolal analysis (eq 3). The solid lines represent the weighted nonlinear least-squares fittings to all of the experimental data for each small solute. All six solute plots in Figure 3 (panels A–F) yield an intercept near -10 and a negative slope. The magnitude of the solute concentration dependence of Γ_{μ_1} ($|\partial\Gamma_{\mu_1}/\partial m_3^\Delta|$) is smallest for glycerol (-11 ; panel A) and largest for glycine betaine (-37 ; panel F) and exhibits the rank order betaine $>$ proline $>$ TMAO $>$ trehalose $>$ K^+Glu^- $>$ glycerol. Column 2 of Table 3 summarizes the data presented in Figure 3.

Determination of Γ_{μ_3} : Γ_{μ_3} Is Proportional to Small Solute Molality. Quantities required to calculate Γ_{μ_3} and Γ_{μ_1,μ_3} from Γ_{μ_1} are collected in Table 2, which summarizes the results of fitting the representative VPO data presented in Figure 1 as well as the densimetry-determined partial molar volumes for each solute. Derivatives with respect to small solute molality of the quadratic functions fitted to the osmolality data, represented by the solid curves in Figure 1, are presented as $(\partial\text{Osm}/\partial m_3)_{m_2=0}$ (column 3) and $(\partial\text{Osm}/\partial m_3)_{[2]}$

Table 3: Summary of Preferential Interaction Coefficients Describing BSA–Small Solute Interactions^a

solute	Γ_{μ_1}	Γ_{μ_3}	$\Gamma_{\mu_1\mu_3}$
glycerol	$-11 \pm 1 - (11 \pm 2)m_3^\Delta$	$-(9.4 \pm 0.4)m_3^*$	$-(10 \pm 1)m_3'$
K ⁺ glutamate	$-8.7 \pm 1.0 - (17 \pm 2)m_3^\Delta$	$-(22 \pm 2)m_3^*$	$-(20 \pm 2)m_3'$
trehalose	$-9.3 \pm 0.6 - (19 \pm 2)m_3^\Delta$	$-(22 \pm 2)m_3^*$	$-(21 \pm 2)m_3'$
TMAO	$-12 \pm 1 - (22 \pm 2)m_3^\Delta$	$-(29 \pm 2)m_3^*$	$-(27 \pm 2)m_3'$
proline	$-9 \pm 1 - (34 \pm 3)m_3^\Delta$	$-(34 \pm 1)m_3^*$	$-(35 \pm 1)m_3'$
betaine	$-10 \pm 1 - (37 \pm 2)m_3^\Delta$	$-(50 \pm 1)m_3^*$	$-(49 \pm 1)m_3'$

^a m_3^Δ , m_3^* , and m_3' are the small solute molalities in the two-component solution (–BSA) under the same thermodynamic constraints as the three-component solution (+BSA) (T, P, μ_1 ; T, P, μ_3 , and T, μ_1, μ_3 , respectively.) Uncertainties reported are from nonlinear least-squares fitting (41) of calculations (cf. eqs 3, 9, 12, and 14) of the preferential interaction coefficients as a function of small solute molality (with a y-intercept of zero for Γ_{μ_3} and $\Gamma_{\mu_1\mu_3}$). Fitting to Γ_{μ_1} was weighted by propagation of the uncertainties in the triplicate osmometry readings and the uncertainty in the quadratic fitting to Osm vs m_3 for the appropriate two-component solutions. Fitting to Γ_{μ_3} was weighted by the uncertainty calculated for each point from the uncertainty in the fittings to Γ_{μ_1} and the fittings to Osm vs m_3 for the appropriate two- and three-component solutions. Fittings to $\Gamma_{\mu_1\mu_3}$ were weighted by the uncertainties in the fittings to Γ_{μ_1} and Γ_{μ_3} .

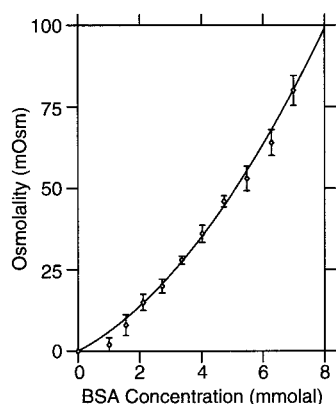


FIGURE 4: Solution osmolality as a function of BSA molality. Error bars represent the standard deviation of triplicate osmometric measurements for each BSA–water solution. The solid curve is the nonlinear least-squares quadratic fitting to the data (see Experimental Procedures).

(column 5). The corresponding solute concentration range examined and the number of individual determinations (each performed in triplicate) are given in columns 4 and 6.

Γ_{μ_3} (defined by eq 4) is calculated according to eq 9 from the osmolality derivatives presented in Table 2 and the fits to Γ_{μ_1} presented in Figure 3 (and column 2 of Table 3). The derivatives in column 5 of Table 2 are at constant protein molarity (cf. Figure 1) and are converted to the same derivative at constant protein molality using eq 17. The data required to obtain $(\partial\text{Osm}/\partial m_2)_{m_3=0}$ are shown in Figure 4, which plots the dependence of osmolality on BSA molality in the absence of any small solute. The derivative of the quadratic fit to the BSA–water data is given in Table 2. In the range of protein molalities represented in Figure 1, the BSA contribution to the solution osmolality (Figure 4) lies between 20 and 40 mOsm, and the derivative of solution osmolality with respect to BSA molality (the slope of the curve in Figure 4) is relatively constant, varying from 9.3 (± 1.3) to 12.7 (± 1.8). At low BSA concentrations, the solution osmolality is 5-fold larger than the ideal contribution of an uncharged protein. This difference must reflect the contribution of any dissociated BSA counterions to the

osmolality of the dialyzed, essentially salt-free BSA solution. BSA has approximately 217 total charges [calculated from the amino acid sequence (35)]. The net charge on BSA estimated from its amino acid composition in the pH range of our experiments could be as large as -17 [-99 from carboxyl groups of aspartates and glutamates; -1 from the C-terminal carboxyl group; $+1$ from the N-terminal amino group; $+59$ from lysines; $+23$ from arginines (35)], reduced in magnitude if any of the 17 histidine residues are protonated. The net charge on human serum albumin was determined by Tanford from analysis of pH titration curves to be approximately -14 at pH 7 (44).

The second method of calculating Γ_{μ_3} , according to eq 12, uses $(\partial\text{Osm}/\partial m_3)_{m_2=0}$ and $(\partial\text{Osm}/\partial m_3)_{m_2}$ [Table 2, columns 3 and 5 (converted using eq 17)]. We have calculated Γ_{μ_3} using the two independent approximations (eqs 8 and 11) individually and together. For all of the solutes we have examined, we find that Γ_{μ_3} does not depend on which (or both) of the two approximations is used and is proportional to small solute molality (m_3^*) within experimental uncertainty. The weighted average of the two independent methods of calculating Γ_{μ_3} as a function of m_3^* (as defined in eq 4) is summarized in column 3 of Table 3. The proportionality constants Γ_{μ_3}/m_3^* vary from -9.4 ± 0.4 (glycerol) to -50 ± 1 (betaine).

Determination of $\Gamma_{\mu_1\mu_3}$: For the Conditions Examined, $\Gamma_{\mu_1\mu_3}$ Is Equal to Γ_{μ_3} and Is Proportional to Small Solute Molality (m_3'). The preferential interaction coefficient that corresponds to the conditions of a dialysis equilibrium, $\Gamma_{\mu_1\mu_3}$, is calculated exactly from values of Γ_{μ_1} (Figure 3; column 1 of Table 3) and Γ_{μ_3} (column 2 of Table 3) and the partial molar volumes of each solute (column 1, Table 2) using eq 14. Figure 5 presents $\Gamma_{\mu_1\mu_3}$ as a function of the calculated molality of the small solute in a two-component solution in dialysis equilibrium with the BSA solution (m_3' , defined in eq 5) and shows the error propagation from the uncertainties in the fitted curves in Figures 1, 3, and 4, as summarized in Tables 2 and 3. For each of the small solutes, we find that $\Gamma_{\mu_1\mu_3}$ is proportional to small solute molality (m_3'). Figure 5 (panels A–F) show a progression in the slopes ($\Gamma_{\mu_1\mu_3}/m_3'$) from glycerol (-10 ± 1) to betaine (-49 ± 1). The solutes K⁺Glu[−] [$-20 (\pm 2)$; panel B], trehalose [$-20 (\pm 2)$; panel C], TMAO [$-27 (\pm 2)$; panel D], and proline [$-35 (\pm 1)$; panel E] exhibit intermediate values of $\Gamma_{\mu_1\mu_3}/m_3'$. For each of these six solutes, the slope of the data in Figure 5 is given in Table 3, column 3.

DISCUSSION

Comparison of Solute–BSA Interactions with Results for Smaller Proteins Leads to the Proposal That $\Gamma_{\mu_1\mu_3}/m_3'$ Is Proportional to Water-Accessible Surface Area (ASA) for a Homologous Series of Native Proteins. The results reported here represent the first systematic characterization of the variation of $\Gamma_{\mu_1\mu_3}$ with small solute concentration for the interactions of *E. coli* osmolytes and other protein-stabilizing solutes with a single native protein (BSA). We find in all cases that $\Gamma_{\mu_1\mu_3}$ is proportional to small solute molality (m_3') up to at least 1 *m*. A previous detailed and systematic study of interactions of trehalose (≤ 0.8 *m*) with ribonuclease A (RNaseA) by equilibrium dialysis and densimetry (45) found that $\Gamma_{\mu_1\mu_3}$ is proportional to trehalose concentration. A

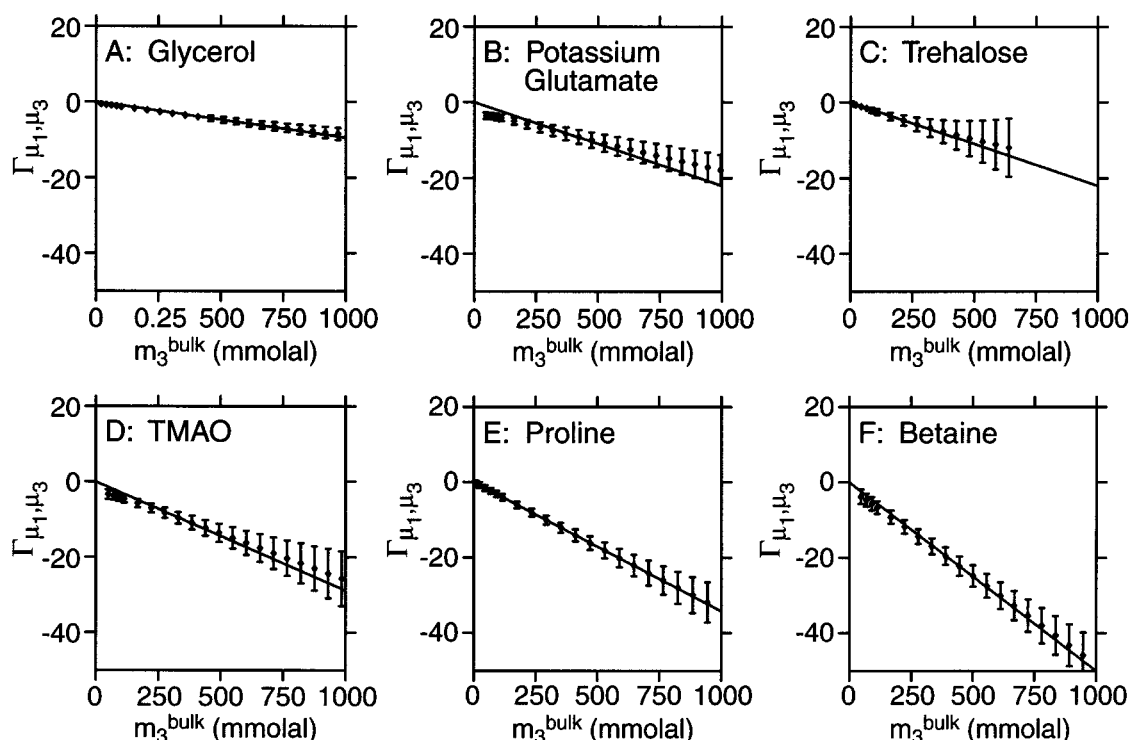


FIGURE 5: Γ_{μ_1, μ_3} as a function of bulk small solute molality. Panels A–F show results for glycerol, K^+Glu^- , trehalose, TMAO, proline, and glycine betaine, respectively. The data points shown are calculated from eq 14. The error bars represent the propagation of the errors reported in Table 2 for the fittings of the osmometry data. The solid line is the least-squares fitting forced to have an intercept of zero.

number of individual dialysis/densimetric determinations of preferential interaction coefficients for various proteins at one or several concentrations of the small solutes investigated here have been reported by Timasheff and co-workers (11, 21, 45–52), but the dependence of Γ_{μ_1, μ_3} on m'_3 generally has not been investigated. Typically, different solution conditions (various types and concentrations of buffer and salt, pH, temperature) were used in the different studies.

Table 4 summarizes our data and that of Timasheff and co-workers as values of $\Gamma_{\mu_1, \mu_3}/m'_3$ and the corresponding weight scale quantity $(g'_3)^{-1}(\partial g_3/\partial g_2)$. To calculate these quantities, literature values of Γ_{μ_1, μ_3} were analyzed assuming that Γ_{μ_1, μ_3} is proportional to the appropriate small solute molality (m'_3), as observed for all solutes investigated here (cf. Figure 5). Table 4 shows that, for each solute, $\Gamma_{\mu_1, \mu_3}/m'_3$ increases systematically with increasing protein size. Preferential interaction coefficients at one or more molalities of four of the solutes investigated here are available for lysozyme (11, 46–48, 50). In addition, several published values of Γ_{μ_1, μ_3} for these solutes with other proteins are included in Table 4 (45, 47–52). (Cases where $\Gamma_{\mu_1, \mu_3}/m'_3$ was calculated from a single solute molality are indicated by footnote *a* in Table 4).

Two alternative normalizations of these data are equally effective in reducing or eliminating the protein size dependence of $\Gamma_{\mu_1, \mu_3}/m'_3$ for a given small solute. If each $\Gamma_{\mu_1, \mu_3}/m'_3$ is divided by the ASA of the protein [calculated (43) using coordinates for protein crystal structures (53–60) from the RCSB Protein Data Bank (61)], the differences between different proteins for interactions with a given solute are greatly reduced, as shown in column 6 of Table 4. Alternatively, the quantity $\Gamma_{\mu_1, \mu_3}/m'_3 = (m'_3)^{-1}(\partial m_3/\partial m_2)_{T, \mu_1, \mu_3}$ may be converted to the corresponding weight concentration scale quantity $(g'_3)^{-1}(\partial g_3/\partial g_2)_{T, \mu_1, \mu_3}$, where g_3 and g_2 are expressed

in grams of each solute per gram of water, and g'_3 is the corresponding weight concentration of small solute in dialysis equilibrium with the protein solution. Because all proteins have similar partial specific volumes, the weight-based normalization⁷ is fundamentally a volume-based normalization of the preferential interaction coefficient. As shown in Table 4, no distinction can be made between volume-based and ASA-based normalizations because of experimental uncertainty and the similarity of surface-to-volume ratios for all of these proteins. However, a clear choice can be made between these normalizations at a molecular level. We propose that both preferential interactions of solutes and hydration of proteins are best analyzed using an ASA-based normalization because the underlying physical phenomena are molecular interactions of solutes and water with protein surface.

Proportionality of Γ_{μ_1, μ_3} to Bulk Small Solute Molality and to Protein Water-Accessible Surface Area Is Predicted by the Local/Bulk Domain Model. The local/bulk model interprets the preferential interaction coefficient in terms of the partitioning of a small solute between a local domain near the biopolymer surface and a bulk domain sufficiently distant from any biopolymer such that the small solutes do not interact with the biopolymer. The two microscopic domains are analogous to the two macroscopic domains (protein–solute–water and solute–water) in an equilibrium dialysis experiment where only water and small solute can diffuse across the membrane (see Background). Experimental values of Γ_{μ_1, μ_3} can be interpreted using the local/bulk model to quantify the extent of small solute accumulation or of

⁷ Weight-based normalizations have been used to report preferential interaction coefficients in many previous studies (21 and references therein).

Table 4: Values of Γ_{μ_1, μ_3} for Native Proteins Can Be Compared When Normalized by m'_3 and ASA as Predicted by the Local/Bulk Model

small solute	protein ^a	ASA ^b $\times 10^{-3}$	molecular mass (kDa)	$-\Gamma_{\mu_1, \mu_3}/m'_3$	$(-\Gamma_{\mu_1, \mu_3}/m'_3 \text{ASA}) \times 10^4$	$-(1/g'_3)(\partial g_3/\partial g_2) \times 10^4$
glycerol	BSA	29	66	10 \pm 1	3.4 \pm 0.3	1.5 \pm 0.3
				12 \pm 1 ^c	4.1 \pm 0.3	1.8 \pm 0.3
	chymotrypsinogen A	11	26	5.8 \pm 0.7 ^d	5.3 \pm 0.6	2.2 \pm 0.3
	α -chymotrypsin	9.3	25	4.4 \pm 0.2 ^d	4.7 \pm 0.2	1.8 \pm 0.1
	β -lactoglobulin	8.2	18	2.4 \pm 0.1 ^d	2.9 \pm 0.1	1.3 \pm 0.1
	lysozyme ^a	6.6	15	1.9 \pm 0.5 ^d	2.9 \pm 0.8	1.3 \pm 0.3
	RNase A	6.9	14	2.0 \pm 0.1 ^d	2.9 \pm 0.1	1.4 \pm 0.1
K ⁺ (or Na ⁺) glutamate	insulin ^a	6.0	11	2.7 \pm 0.4 ^d	4.5 \pm 0.7	2.5 \pm 0.4
	BSA	29	66	20 \pm 2	6.9 \pm 0.7	3.0 \pm 0.3
				30 \pm 2 ^e	10 \pm 1	4.5 \pm 0.3
	tubulin	19	49	12 \pm 3 ^e	6.3 \pm 1.6	2.4 \pm 0.6
	β -lactoglobulin	8.2	18	8.6 \pm 0.8 ^e	10 \pm 1	4.8 \pm 0.4
	lysozyme ^a	6.6	15	5.1 \pm 0.2 ^e	7.7 \pm 0.3	3.4 \pm 0.1
	BSA	29	66	21 \pm 2	7.2 \pm 0.7	3.2 \pm 0.3
trehalose	RNaseA	6.9	14	7.3 \pm 0.2 ^f	11 \pm 1	5.2 \pm 0.1
	BSA	29	66	27 \pm 2	9.3 \pm 0.7	4.1 \pm 0.3
TMAO	RNase T1	5.4	11	6 \pm 2 ^g	11 \pm 4	5.5 \pm 1.8
	BSA	29	66	35 \pm 1	12 \pm 0.3	5.3 \pm 0.2
proline	lysozyme ^a	6.6	15	5 \pm 1 ^h	7.6 \pm 1.5	3.3 \pm 0.7
	BSA	29	66	50 \pm 1	17 \pm 0.3	7.6 \pm 0.2
betaine				32 \pm 7 ⁱ	11 \pm 2	4.8 \pm 1.1
	lysozyme	6.6	15	6 \pm 2 ⁱ	9.1 \pm 3	4.0 \pm 1.3

^a For these proteins, preferential interaction coefficients were determined at only one small solute concentration. ^b ASA is the water accessible surface area of the protein calculated as described in ref 41. PDB files (61) used for the calculations are 2CGA for chymotrypsinogen A (53); 4CHA for α -chymotrypsin (54); 1B0O for β -lactoglobulin (55); 6LYZ for lysozyme (56); 3RN3 for RNaseA (57); 2INS for insulin (58); 1TUB for tubulin (59); and 9RNT for RNaseT1 (60). ^c Calculated from data of Gekko and Morikawa (49). ^d Calculated from data of Gekko and Timasheff (50). ^e Calculated from data of Arakawa and Timasheff (48). ^f Calculated from data of Xie and Timasheff (45) and Lin and Timasheff (52). ^g Calculated from data of Lin and Timasheff (51). ^h Calculated from data of Arakawa and Timasheff (11, 46). ⁱ Calculated from data of Arakawa and Timasheff (47).

exclusion in the local domain in terms of a solute-binding constant (20, 24, 31) or a solute partition coefficient, introduced below.

For a nonelectrolyte solute, a thermodynamically rigorous analysis of the local–bulk domain model by Record and Anderson (20, 28) yields the result

$$\Gamma_{\mu_1, \mu_3} = B_3 - m_3^{\text{bulk}} B_1 / m_1 \quad (18)$$

For a 1:1 electrolyte solute in a solution with an anionic biopolymer, the corresponding result for the preferential interaction coefficient of the salt component, which is equal to that of the salt anion, is (20, 28)

$$\Gamma_{\mu_1, \mu_3} = \Gamma_- = -0.5(|Z_P| - B_+ - B_-) - m_3^{\text{bulk}} B_1 / m_1 \quad (19)$$

In eqs 18 and 19, B is the average number of molecules of the indicated component in the local domain (expressed per biopolymer molecule), m_3^{bulk} is the molal concentration of the solute component in the bulk domain, $|Z_P|$ is the net charge on the protein. Here we define a local–bulk partition coefficient K_P for a nonelectrolyte solute (or each ion of an electrolyte solute) as

$$K_P \equiv \frac{(n_3/n_1)^{\text{local}}}{(n_3/n_1)^{\text{bulk}}} = \frac{(B_3/B_1)}{(m_3^{\text{bulk}}/m_1)} \quad (20)$$

where n_3 and n_1 are the number of moles of small solute and water, respectively, in the indicated domain. We propose that a partition coefficient K_P is more suitable than a solute–protein binding constant because the observed proportionality of Γ_{μ_1, μ_3} to m_3^{bulk} is most simply interpreted in

terms of a constant K_P (independent of m_3^{bulk}) and because no evidence for saturation of these solute effects at high solute concentration has been obtained here or previously. In addition, we assume that none of the solutes of interest here accumulate to a sufficient extent in the local domain to reduce B_1 appreciably from B_1^0 , the amount of water in the local domain in the absence of solute [i.e., $m_3^{\text{bulk}} S_{1,3}/m_1 \ll 1$, where $S_{1,3}$ is the stoichiometry of the local solute–water exchange process (28)]. We assume that B_1^0 is proportional to the ASA of the biopolymer. From the thermodynamic analysis of the local–bulk domain model, it can be shown that $m_3^{\text{bulk}} = m'_3$ (20, 28). Therefore, for an uncharged solute, eqs 18 and 20 can be combined to give

$$\frac{\Gamma_{\mu_1, \mu_3}}{m'_3(\text{ASA})} = \frac{(K_P - 1)b_1^0}{m_1} \quad (21)$$

where b_1^0 is the amount of water in the local domain expressed as molecules of water per \AA^2 of biopolymer surface. For a 1:1 electrolyte and a weakly charged protein, so that $|Z_P|$ is negligible in comparison to Γ (28), then

$$\frac{\Gamma_{\mu_1, \mu_3}}{m'_3(\text{ASA})} \cong \frac{[0.5(K_{P,+} + K_{P,-}) - 1]b_1^0}{m_1} \quad (22)$$

The local–bulk domain model, together with the assumption that the solute partition coefficient is independent of bulk solute concentration, therefore predicts that Γ_{μ_1, μ_3} should be proportional to m'_3 (or m_3^{bulk}) and to biopolymer ASA for members of a homologous series (i.e., native proteins, with sufficiently similar distributions of polar and nonpolar surface

residues). The first of these predictions ($\Gamma_{\mu_1, \mu_3} \propto m_3'$ at constant ASA) is verified by the data of Figure 5 (see column 3 of Table 3); the second prediction ($\Gamma_{\mu_1, \mu_3} \propto \text{ASA}$ at constant m_3') is consistent with the data of Table 4 for proteins of different ASA. The data of Table 4 do not indicate whether these native proteins behave as members of one homologous series or whether the differences in surface area characteristics (differences in the fractions of charged, polar, and nonpolar surface) are significant. For example, assuming that the three-dimensional structure of BSA is the same as that of HSA and replacing surface residues based on comparison of the primary sequences, we find that the ASA of BSA is 53% nonpolar, 29% charged and 18% uncharged polar surface, whereas the average native protein ASA is 57% nonpolar, 19% charged, and 24% uncharged polar surface (62). Also the percentage of completely (>95%) buried (water inaccessible) residues in BSA (23%) is significantly smaller than the average for other large native proteins [32%; (62)].

To use eqs 21 and 22 to determine local–bulk partition coefficients K_P (or $K_{P,+}$, $K_{P,-}$) for the solutes investigated here, an independent determination of b_1° is required. Alternatively, to determine b_1° from eq 21 or 22, a completely excluded solute ($K_P = 0$) would be needed. Although independent evidence for the extent of exclusion of any of these solutes from protein surface is not available, values of Γ_{μ_1, μ_3} for the most excluded solute (glycine betaine) provide a minimum estimate of b_1° , as described below.

Γ_{μ_1, μ_3} for Glycine Betaine Provides a Minimum Estimate of the Hydration of BSA (B_1°). The amount of water in the local domain (B_1°) as obtained from the local–bulk domain analysis of Γ_{μ_1, μ_3} is

$$B_1^\circ = m_1 \left(\frac{B_3}{m_3^{\text{bulk}}} - \frac{\Gamma_{\mu_1, \mu_3}}{m_3^{\text{bulk}}} \right) = \frac{m_1}{(K_P - 1)m_3^{\text{bulk}}} \Gamma_{\mu_1, \mu_3} \quad (23)$$

To determine B_1° from measurement of Γ_{μ_1, μ_3} as a function of m_3^{bulk} requires independent knowledge of K_P . Otherwise, a lower-bound estimate of B_1° for BSA is obtained by assuming that $B_3 = 0$ (i.e., $K_P = 0$) for the most excluded solute investigated (glycine betaine), for which we find that $\Gamma_{\mu_1, \mu_3}/m_3^{\text{bulk}} = -49 \pm 1$. From eq 23, we obtain $B_1^\circ \geq 2.8 \times 10^3 \text{ H}_2\text{O/BSA}$ or $b_1^\circ \geq 0.097 \text{ H}_2\text{O}/\text{\AA}^2$ of BSA surface. If the packing density of a monolayer of hydration water is the same as that for bulk water, then $b_1^\circ \cong 0.11 \text{ H}_2\text{O}/\text{\AA}^2$ (63), which corresponds to $B_1^\circ = 3.2 \times 10^3$ water molecules/BSA. NMR relaxation measurements on water in BSA solutions by Torres et al. (64) yield an estimate of $(3.0 \pm 0.2) \times 10^3$ weakly bound waters of hydration [and a small number (one to thirty) of more strongly bound water molecules].

As a working hypothesis, we therefore propose that the local domain in the local–bulk domain model corresponds to the water of biopolymer hydration and that for BSA (and presumably other native proteins) this corresponds to a monolayer coverage of the water accessible surface (i.e., $b_1^\circ = 0.11 \text{ H}_2\text{O}/\text{\AA}^2$ or $B_1^\circ = 3.2 \times 10^3 \text{ H}_2\text{O/BSA}$). Using this interpretation, glycine betaine is highly but not completely excluded from this hydration monolayer.

Timasheff and co-workers have interpreted $-55.5\Gamma_{\mu_1, \mu_3}/m_3$ for a variety of solutes as the amount of protein

Table 5: Solute Distribution in a BSA Solution Assuming the Local Domain Is a Monolayer of Hydration ($1 \text{ H}_2\text{O}/9 \text{ \AA}^2$)

solute	$\Gamma_{\mu_1, \mu_3}/m_3'^a$	K_P^b	B_3^c
randomly distributed limit	0	1.0	58
glycerol	−10	0.83	48
K^+Glu^-	−20	0.65 ^d	37 ^e
trehalose	−21	0.64	37
TMAO	−27	0.53	31
proline	−35	0.39	22
betaine	−50	0.14	8
completely excluded limit	−59	0	0

^a $\Delta\Gamma_{\mu_1, \mu_3}/m_3' \cong B_3/m_3' - B_1^\circ/m_1$. ^b ($K_P = m_3^{\text{local}}$ when $m_3^{\text{bulk}} = 1$); $m_3^{\text{local}} = B_3/(B_1^\circ/M_1)$. ^c At $m_3^{\text{bulk}} = 1 \text{ m}$; $B_1^\circ = 3.2 \times 10^3$. ^d 0.5 ($K_{P,+} + K_{P,-}$) assuming $|Z_P|$ is negligibly small (cf. eq 19). ^e 0.5 ($B_+ + B_-$).

preferential hydration (21). Equation 23 shows that this approach is valid only for highly excluded solutes such as glycine betaine where K_P and hence B_3 are near zero. Published estimates (65–71) of protein hydration from studies with glycerol, trehalose, and other solutes for which $B_3 > 0$ (i.e., $K_P > 0$) provide only imprecise lower bounds on the amount of hydration.

Local–Bulk Partition Coefficients for Solutes in a BSA Solution. Subject to the assumption that the local domain surrounding BSA is a monolayer of hydration water ($B_1 = 3.2 \times 10^3 \text{ H}_2\text{O}$), local–bulk partition coefficients for solutes are readily calculated from eqs 21 and 22. These predictions are given in Table 5. For a 1 m solution of a uniformly distributed solute (for which Γ_{μ_1, μ_3} is zero and independent of m_3^{bulk} , $K_P = 1$ and $m_3^{\text{bulk}} = m_3^{\text{local}}$), an average of 58 solute molecules are predicted per BSA in the local domain ($B_3 = 58$). For a completely excluded solute, $\Gamma_{\mu_1, \mu_3}/m_3^{\text{bulk}} = -58$, $K_P = 0$, and $B_3 = m_3^{\text{local}} = 0$ at any m_3^{bulk} .

All solutes investigated here fall between these two extremes. Partition coefficients of the nonelectrolytes range from 0.83 (glycerol) to 0.14 (betaine). For K^+Glu^- , the analysis is more complicated. Using eq 22 to interpret the K^+Glu^- data, we obtain $K_{P,+} + K_{P,-} \cong 1.3$. If partitioning of the two ionic species K^+ and Glu^- were the same, so that $K_{P,+} = K_{P,-} = 0.65$, then both ions partition like trehalose ($K_P = 0.64$) and are moderately excluded from BSA. However, the placement of Glu^- with F^- , sulfate, and other Hofmeister anions (72–74) that drive processes reducing the exposure of protein surface to water (72) indicates that Glu^- is highly excluded from protein surface, whereas K^+ is in the middle of the corresponding Hofmeister cation series (72) and so is presumably neither strongly accumulated nor excluded. On this basis, we predict that the correct interpretation of the K^+Glu^- data is to set $K_{P,+} \cong 1$, whereby we calculate $K_{P,-} = 0.3$, making glutamate second only to betaine in its exclusion from the local domain in a BSA solution. Experiments with other Hofmeister salts are in progress to test this interpretation.

In Vivo Implications of Solute Exclusion for Osmoprotection. In exponential growth in minimal medium, the concentration of biopolymers in the *E. coli* cytoplasm exceeds 250 mg/mL in cells grown at low external osmolality and increases with increasing osmolality (9). Direct experimental determinations of free and bound water in the *E. coli* cytoplasm show that the ratio of bound water of biopolymer hydration (i.e., the local domain) to free (bulk) water is approximately 0.2 at low external osmolality (0.3 Osm) and

increases to 0.5 at higher osmolality (1.0 Osm) (9, 10, 18). Because local water of biopolymer hydration is such a large fraction of total water, the partitioning of a solute between local and bulk water must have very significant effects on the ability of a given amount of that solute to increase the osmolality of the cytoplasm (9, 10). The extent of partitioning of the solute is also of great significance for predicting the solute concentration dependence of the thermodynamics of biopolymer processes in vivo. In this section, we discuss how solute partitioning affects the osmolality of the cytoplasm and in particular discuss the effect of *E. coli* osmoprotectants. In the following section we consider the perturbing effects of changes in the nature or concentration of excluded solutes, including all *E. coli* osmolytes except K^+ , on biopolymer processes.

Cayley and co-workers previously determined amounts of cytoplasmic water and osmotically significant solutes in *E. coli* for three conditions at high external osmolality (1.0 Osm): (1) growth at 1.0 Osm in a minimal medium; (2) growth at 1.0 Osm in the presence of 1 mM proline; (3) growth at 1.0 Osm in the presence of 1 mM betaine (9, 10, 18). In exponential growth at 1.0 Osm, the primary osmolytes are K^+Glu^- and trehalose and the amount of free cytoplasmic water is approximately $0.8 \mu\text{L}/\text{mg}$ dry weight. If an osmoprotectant (proline or glycine betaine) is present in the growth medium, it is transported into the cytoplasm, replacing much of the K^+Glu^- and trehalose, and increasing the volume of free water and the growth rate. Betaine allows the uptake of more water and a higher growth rate than does proline.

Assuming additivity of the effects of the individual osmolytes, we estimate the contribution of these osmolytes to the effective cytoplasmic preferential interaction coefficient as the sum

$$\Gamma_{\text{cyto}} = \sum \Gamma_{\mu_1, \mu_3} \quad (24)$$

where Γ_{μ_1, μ_3} is determined for each osmolyte by calculating m_3^{bulk} based on the partitioning of each osmolyte (using K_P ; cf. Table 5) between free cytoplasmic water and water of biopolymer hydration and on the measured amounts of cellular osmolytes and water (10). [The contribution from K^+Glu^- was estimated from the known concentration of glutamate in the cell (10); the remaining potassium ions (which neutralize much of the nucleic acid phosphate charge) are not included in this calculation.] Cayley and co-workers have already shown that growth rate increases with free cytoplasmic water volume (V_f) and that a tradeoff between K^+ and V_f provides a balance of perturbing effects on protein–nucleic acid interactions (9). Figure 6 shows that a direct, approximately linear, correlation also exists between Γ_{cyto} and V_f . Exclusion of a solute from protein ASA effectively concentrates that solute in the bulk cytoplasmic water, resulting in a higher osmolality than for the same amount of a less excluded solute (cf. Figure 2). In other words, a lower total concentration of an excluded solute (than of a randomly distributed or accumulated solute) is required to match the cytoplasmic osmolality with that of the high osmolality of the cell's environment. Transport and/or synthesis of a given amount of a solute allows a larger cytoplasmic water volume (greater V_f) and a faster growth rate if it is excluded from biopolymer ASA.

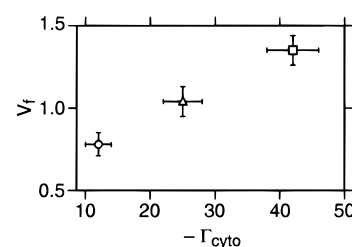


FIGURE 6: Free cytoplasmic water volume (V_f) for cells grown in 1 Osm minimal medium as a function of the cytoplasmic preferential interaction coefficient (cf. eq 24). The circle represents cells grown without added osmoprotectants. The triangle represents cells grown in the presence of 1 mM proline. The square represents cells grown in the presence of 1 mM glycine betaine. Error bars include the error in free cytoplasmic water volume (10) and errors for the individual solute Γ_{μ_1, μ_3} (cf. Table 3).

Implications of Osmolyte–BSA Thermodynamics for Interpretation of in Vitro “Osmotic Stress” Experiments. Consider, for simplicity, a biopolymer process which can be modeled as docking of rigid interfaces and in which no coupled equilibria (e.g., aggregation, dissociation of subunits) are present. For this case, an increase in the concentration of a solute which is excluded from the local water of hydration of all biopolymer participants in a biopolymer process (all $\Gamma_{\mu_3} < 0$ and $K_P < 1$) will drive the process in the direction that reduces total biopolymer ASA. Such excluded solutes have been shown to stabilize native proteins (1, 11–13, 21, 45–52) and their assemblies (22, 71) that expose less ASA than the respective denatured or unassembled states. If a solute were *completely* excluded from the water of hydration of the molecular surfaces that interact in a process (all $K_P = 0$), such a solute would be useful as a direct probe of changes in hydration in that process (cf. eqs 1 and 23). However, if the solute is not completely excluded, its use in an “osmotic stress” experiment will lead to an underestimate of the magnitude of the change in hydration unless a more complete preferential interaction analysis is used to interpret the data.

The “osmotic stress” approach (22) has recently been widely applied to analyze effects of solute concentration on the thermodynamics ($\Delta G_{\text{obs}}^\circ$ or K_{obs}) of a variety of biopolymer processes: protein–DNA interactions (65–70, 75); protein–protein interactions (71, 76); protein conformational changes (77–79); enzymatic reactions (80, 81), and protein–membrane interactions (80). Interpretation of these “osmotic stress” experiments has been based on a model in which the effect of solute concentration on biopolymer processes arises from the existence of solute-inaccessible regions of water at or near the surface of the biopolymer (22). The reduction in water activity which occurs upon the addition of solute is interpreted as an “osmotic stress”, driving biopolymer processes (conformational change, binding or assembly) in the direction which releases water. In these experiments, the effect of changing osmolality (by addition of the solute) on the equilibrium constant of a biopolymer process is measured, and interpreted in the “osmotic stress” analysis, as

$$\frac{\partial \ln K_{\text{obs}}}{\partial \text{Osm}} = -\Delta n_1 / 55.5 \quad (25)$$

where Δn_1 is the change in the amount of “solute-inaccessible” water in the process. However, unless the solute is

completely excluded from the water of hydration of all of the biopolymer surface affected (i.e., buried or exposed) in the process, the effect on K_{obs} of changes in small solute concentration will include contributions from biopolymer–solute interactions as well as biopolymer–water interactions (as described below).

For the usual experimental situation in which the concentration of added solute greatly exceeds the concentrations of the interacting biopolymers, the fundamental Gibbs–Duhem relationship for a two-component solution (at constant temperature and pressure) is applicable:

$$d\text{Osm} = -55.5 d \ln a_1 = m_3 d \ln a_3 \quad (26)$$

Therefore the “osmotic stress” derivative $\partial \ln K_{\text{obs}}/\partial \text{Osm}$ is equivalent to that in eq 1:

$$\left(\frac{\partial \ln K_{\text{obs}}}{\partial \text{Osm}} \right)_{T,P,m_2 \rightarrow 0} = \frac{1}{m_3} \left(\frac{\partial \ln K_{\text{obs}}}{\partial \ln a_3} \right)_{T,P,m_2 \rightarrow 0} \cong \frac{\Delta \Gamma_{\mu_3}}{m_3} \quad (27)$$

Table 3 demonstrates that values of Γ_{μ_3}/m_3 for the interactions of different “osmotic stress” solutes with native protein surface are different and that common osmotic stress solutes such as glycerol and sugars are far from the excluded solute limit necessary for a direct interpretation of $(\partial \ln K_{\text{obs}}/\partial \text{Osm})$ as the stoichiometry of participation of water.

The local–bulk domain interpretation (eq 21) can be used to show explicitly the effect of solute partitioning on $(\partial \ln K_{\text{obs}}/\partial \text{Osm})$:

$$\frac{\partial \ln K_{\text{obs}}}{\partial \text{Osm}} = \frac{1}{55.5} \Delta[B_1^0(K_p - 1)] \quad (28)$$

Only if $K_p = 0$ for the interactions of the solute (used to change solution osmolality) with all regions of biopolymer surface affected by the process does $(\partial \ln K_{\text{obs}}/\partial \text{Osm}) = -\Delta B_1^0/55.5$, the traditional “osmotic stress” interpretation. For a hypothetical process that buries 10^3 \AA^2 of ASA and releases ~ 100 waters of hydration ($\Delta B_1^0 = -100$), eq 28 predicts for glycerol ($K_p = 0.83$) that $(\partial \ln K_{\text{obs}}/\partial \text{Osm}) = 17/55.5$ or (using eq 25) $\Delta n_1 = -17$. An osmotic stress interpretation of this result might be that, on average, only 17% of the interacting surface is glycerol-inaccessible due to preferential exclusion. Regardless of the molecular-level picture invoked to explain the observed preferential interaction of glycerol with protein ASA, it is clear that an interpretation of $(\partial \ln K_{\text{obs}}/\partial \text{Osm})$ assuming complete exclusion of glycerol from all interacting regions of the proteins would give an extreme underestimate of the magnitude of the total number of water molecules released and the total ASA buried. Changes in K_{obs} (and ΔG_{obs}^0) with respect to changes in water activity therefore depend both on changes in hydration (ΔB_1) of the products and reactants and on the small solute partitioning between bulk and hydration domains (incorporated in K_p , cf. eq 20).

We have shown in this study that osmolytes are excluded to varying extents from the local domains of water of hydration of native BSA. If the hydration of BSA is a monolayer of $\sim 3.2 \times 10^3$ water molecules (see above and ref 64), only betaine appears to be almost completely excluded from this water. Therefore, when any of the other solutes (e.g., glycerol) is used as a probe of changes in

macromolecular hydration, applying the “osmotic stress” analysis will underestimate the total number of water molecules released in a process (or overestimate the number taken up), as well as the change in ASA. Any interaction between macromolecular surfaces that involves release of water of hydration will also release any small solute molecules present in the water of hydration, and must be analyzed using preferential interaction coefficients.

ACKNOWLEDGMENT

We would like to thank Ruth M. Saecker for helpful discussions, editing of the manuscript, and assistance with protein surface area calculations. We would also like to thank Laura Vanderploeg for preparation of the figures and Sheila Aiello for assistance in preparation of the manuscript. Helpful critique of the manuscript was also given by several members of this laboratory.

APPENDIX 1

Relationship between Constant Water and Constant Solute Chemical Potential Preferential Interaction Coefficients. To derive eq 6 relating Γ_{μ_1} (cf. eq 3) and Γ_{μ_3} (cf. eq 4), the three-component Gibbs–Duhem equation at constant temperature and pressure is used to obtain the following two relationships between derivatives of the solute chemical potentials:

$$-m_1(\partial \mu_1/\partial m_2)_{m_3} = m_2(\partial \mu_2/\partial m_2)_{m_3} + m_3(\partial \mu_3/\partial m_2)_{m_3} \quad (\text{A1})$$

$$-m_1(\partial \mu_1/\partial m_3)_{m_2} = m_2(\partial \mu_2/\partial m_3)_{m_2} + m_3(\partial \mu_3/\partial m_3)_{m_2} \quad (\text{A2})$$

(To simplify the notation, the subscripts indicating constant T and P in these partial derivatives have been omitted.) After division of eq A1 by eq A2 and introduction of the definitions of Γ_{μ_1} and Γ_{μ_3} , we obtain

$$\begin{aligned} \Gamma_{\mu_3} &= [\Gamma_{\mu_1} + (m_2(\partial \mu_2/\partial m_2)_{m_3}/m_3(\partial \mu_3/\partial m_3)_{m_2})] / \\ &\quad [(m_2\Gamma_{\mu_1}/m_3) + 1] \\ &= (\Gamma_{\mu_1} + Q) / [(m_2\Gamma_{\mu_1}/m_3) + 1] \end{aligned} \quad (6)$$

where the quotient Q is defined in eq 7 in the text.

In our previous analyses of osmometric data on BSA solute systems (29), Q in eq 6 was simplified by taking the limit as protein concentration goes to zero. We have since found (using equipment that was not available at the time of the previous study) that even in the limit of zero protein concentration, $m_2(\partial \mu_2/\partial m_2)/RT$ is not equal to 1 because of the contribution of dissociated counterions to the chemical potential of BSA. Moreover, the protein concentrations investigated by VPO are high enough so that $(\partial \mu_2/\partial m_2)$ exhibits a significant dependence on m_2 (Figure 4). We determined this derivative by fitting plots of Osm vs m_2 for solutions containing no solute, measured using the VAPRO 5520 osmometer. Such measurements were not possible on the earlier generation 5500 osmometer used by Zhang et al. (29).

Conversion of Osmolality Dependence on Small Solute Molality at Constant Protein Molality to That at Constant Protein Molality. Three-component solutions were prepared for osmometry experiments at constant BSA molality for

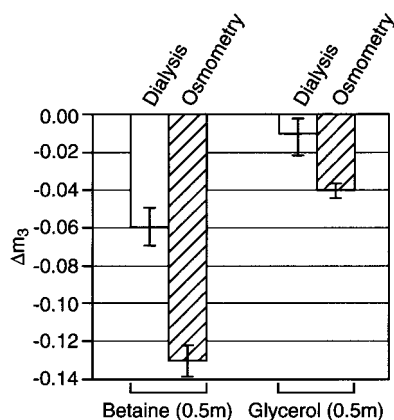


FIGURE 7: Differences between two-component and three-component small solute molalities calculated for dialysis (T, μ_1, μ_3 constant) and for osmometry (T, P, μ_1 constant) for glycine betaine and for glycerol (cf. eqs 3 and 5). Error bars are calculated from the error on Γ_{μ_1} and Γ_{μ_1, μ_3} (cf. Table 3).

experimental convenience, but it is the dependence of osmolality on small solute molality at constant protein molality that is needed in evaluating Γ_{μ_3} from the osmometry data using eqs 9 or 12. For a three component solution, the chemical potential of water at constant temperature and pressure can be differentiated with respect to small solute molality at constant protein molality to yield

$$(\partial \mu_1 / \partial m_3)_{[2]} = (\partial \mu_1 / \partial m_2)_{m_3} (\partial m_2 / \partial m_3)_{[2]} + (\partial \mu_1 / \partial m_3)_{m_2} \quad (\text{A3})$$

The partial derivative of the protein molality with respect to the small solute molality at constant protein molarity can be expressed as a ratio of the dependences of protein molarity on the molality of the two solute components by using the cyclic rule

$$(\partial m_2 / \partial m_3)_{[2]} = -(\partial [2] / \partial m_3)_{m_2} / (\partial [2] / \partial m_2)_{m_3} \quad (\text{A4})$$

The two derivatives on the right-hand side of eq A4 can be expressed in terms of the solute partial molar volumes (29):

$$(\partial m_2 / \partial m_3)_{[2]} = ([2] \bar{V}_3) / (1 - [2] \bar{V}_2) \quad (\text{A5})$$

Substituting this and the definition of Γ_{μ_1} (eq 3) back into eq A3 and solving for $(\partial \mu_1 / \partial m_3)_{m_2}$ yields eq 17.

APPENDIX 2

Advantages of the VPO Approach. Although determination of Γ_{μ_1} and conversion to Γ_{μ_1, μ_3} may seem less direct and therefore possibly subject to greater experimental uncertainty than a direct determination of Γ_{μ_1, μ_3} using equilibrium dialysis, we propose that the VPO approach to determining Γ_{μ_1, μ_3} is preferable for the following reasons. (1) The signal-to-noise ratio in determining the difference in small solute molality in the presence and absence of protein under the constraints appropriate for the preferential interaction coefficient being measured is significantly greater for the VPO measurements. Examples of the molality differences for the two methods are represented in Figure 7 for a three-component solution at a BSA concentration of 3 mM and a total small solute concentration of 0.5 M for the solutes whose effects are at either end of the range examined: betaine and

glycerol. If values calculated for Γ_{μ_3} are independent of the approximation (eq 9 or 12) used to analyze the VPO data, no significant error is introduced in the evaluation of Γ_{μ_1, μ_3} (eq 14) from VPO data. Hence, VPO can be significantly more sensitive for determining Γ_{μ_1, μ_3} than direct measurement by equilibrium dialysis. (2) In the osmometry experiments, the protein and solute concentrations can be known to very high accuracy, but in a dialysis/densimetry experiment, the protein concentration (and in some cases the solute concentration) is not fixed and must be determined at dialysis equilibrium. The presence of a high concentration of small solute can significantly affect spectrophotometric determinations of protein concentration by affecting both the extinction coefficient and the signal-to-noise ratio of the measurement (49). (3) Osmometry experiments do not require large solution volumes. In order for the molality of the small solute in the dialyzing solution to remain constant at its initial value over the course of the dialysis experiment, as indicated in published protocols for using densimetry in combination with equilibrium dialysis (21, 45–52), the volume of the dialyzing solution must be in great excess over the combined volume of all of the protein solutions with which it is in dialysis equilibrium.

REFERENCES

- Yancey, P. H., Clark, M. E., Hand, S. C., Bowlus, R. D., and Somero, G. N. (1982) *Science* 217, 1214–1222.
- Strøm, A. R., Falkenberg, P., and Landfald, B. (1986) *FEMS Microbiol. Rev.* 39, 79–86.
- Van Laere, A. (1989) *FEMS Microbiol. Rev.* 63, 201–210.
- Christian, J. H. B. (1955) *Aust. J. Biol. Sci.* 8, 75–82.
- Tempest, D. W., Meers, J. L., and Brown, C. M. (1970) *J. Gen. Microbiol.* 64, 171–185.
- Measures, J. C. (1975) *Nature* 257, 398–400.
- LeRudulier, D., Strøm, A. R., Dandekar, A. M., Smith, C. T., and Valentine, R. C. (1984) *Science* 224, 1064–1068.
- Whatmore, A. M., Chudek, J. A., and Reed, R. H. (1990) *J. Gen. Microbiol.* 136, 2527–2535.
- Cayley, D. S., Lewis, B. A., Guttman H. J., and Record, M. T., Jr. (1991) *J. Mol. Biol.* 222, 281–300.
- Cayley, D. S., Lewis, B. A., and Record, M. T., Jr. (1992) *J. Bacteriol.* 174, 1586–1595.
- Timasheff, S. N. (1992) in *Water and Life: Comparative Analysis of Water Relationships at the Organismic, Cellular, and Molecular Levels* (Somero, G. N., Osmond, C. B., and Bolis, G. L., Eds.) pp 70–84, Springer-Verlag, Berlin.
- Galinski, E. A. (1993) *Experientia* 49, 487–496.
- Kempf, B., and Bremer, E. (1998) *Arch. Microbiol.* 170, 319–330.
- Rhodes, D., and Hanson, A. D. (1993) *Annu. Rev. Plant. Physiol. Plant. Mol. Biol.* 44, 357–384.
- Jones, R. G. W., Storey, R., Leigh, R. A., Ahmad, N., and Pollard, A. (1977) in *Regulation of Cell Membrane Activities in Plants* (Morre, E., and Ciferri, O., Eds.) p 121, Elsevier, Amsterdam.
- Lang, F., Busch, G. L., and Volkl, H. (1998) *Cell. Physiol. Biochem.* 8, 1–45.
- Burg, M. B. (1997) *Curr. Opin. Nephrol. Hypertens.* 6, 430–433.
- Record, M. T., Jr., Courtenay, E. S., Cayley, D. S., and Guttman H. J. (1998) *Trends Biochem. Sci.* 23, 143–149.
- Record, M. T., Jr., Courtenay, E. S., Cayley, D. S., and Guttman H. J. (1998) *Trends Biochem. Sci.* 23, 190–194.
- Record, M. T., Jr., Zhang, W., and Anderson, C. F. (1998) *Adv. Protein Chem.* 51, 281–353.
- Timasheff, S. N. (1998) *Adv. Protein Chem.* 51, 355–433.
- Parsegian, V. A., Rand, R. P., and Rau, D. C. (1995) *Methods Enzymol.* 259, 43–94.

23. Baskakov, I., and Bolen, D. W. (1998) *J. Biol. Chem.* 273, 4831–4834.
24. Schellman, J. A. (1990) *Biophys. Chem.* 37, 121–140.
25. Low, P. S. (1985) in *Transport Processes, Iono- and Osmoregulation* (Gilles, R., and Gilles-Baillien, M., Eds.) p 471, Springer-Verlag, Berlin.
26. Capp, M. W., Cayley, D. S., Zhang, W., Guttman, H. J., Melcher, S. E., Saecker, R. M., Anderson C. F., and Record, M. T., Jr. (1996) *J. Mol. Biol.* 258, 25–36.
27. Timasheff, S. N. (1998) *Proc. Natl. Acad. Sci. U.S.A.* 95, 7363–7367.
28. Record, M. T., Jr., and Anderson, C. F. (1995) *Biophys. J.* 68, 786–794.
29. Zhang, W., Capp, M. W., Bond, J. P., Anderson, C. F., and Record, M. T., Jr. (1996) *Biochemistry* 35, 10506–10516.
30. Eisenberg, H. (1976) *Biological Macromolecules and Polyelectrolytes in Solution*, Clarendon Press, Oxford.
31. Tanford, C. (1969) *J. Mol. Biol.* 39, 539–544.
32. Wyman, J. (1964) *Adv. Protein Chem.* 19, 223–286.
33. Anderson, C. F., and Record, M. T., Jr. (1993) *J. Phys. Chem.* 97, 7116–7126.
34. Eisenberg, H. (1994) *Biophys. Chem.* 53, 57–68.
35. Peters, T., Jr., Ed. (1996) in *All About Albumin: Biochemistry, Genetics, and Medical Applications*, Academic Press, San Diego.
36. Anderson, C. F., Courtenay, E. S., and Record, M. T., Jr. (1999) *J. Phys. Chem.* (submitted for publication).
37. Lide, D. R., Ed. (1990) in *CRC Handbook of Chemistry and Physics* pp CRC, Boca Raton, FL.
38. Mach, H., Middaugh, C. R., and Lewis, R. V. (1992) *Anal. Biochem.* 260, 74–80.
39. Baldwin, R. L. (1957) *Biochem. J.* 65, 503–512.
40. Squire, P. G., Moser, P., and O'Konski, C. T. (1968) *Biochemistry* 7, 4261–4272.
41. Johnson, M. L., and Frasier, S. G. (1985) *Methods Enzymol.* 117, 301–342.
42. He, X. M., and Carter, D. C. (1992) *Nature* 358, 209–215.
43. Livingstone, J. R., Spolar, R. S., and Record, M. T., Jr. (1991) *Biochemistry* 30, 4237–4244.
44. Tanford, C. (1950) *J. Am. Chem. Soc.* 72, 441–451.
45. Xie, G., and Timasheff, S. N. (1997) *Biophys. Chem.* 64, 25–43.
46. Arakawa, T., and Timasheff, S. N. (1985) *Biophys. J.* 47, 411–414.
47. Arakawa, T., and Timasheff, S. N. (1983) *Arch. Biochem. Biophys.* 224, 169–177.
48. Arakawa, T., and Timasheff, S. N. (1984) *J. Biol. Chem.* 259, 4979–4986.
49. Gekko, K., and Morikawa, T. (1981) *J. Biochem.* 90, 39–50.
50. Gekko, K., and Timasheff, S. N. (1981) *Biochemistry* 20, 4667–4676.
51. Lin, T., and Timasheff, S. N. (1994) *Biochemistry* 33, 12695–12701.
52. Lin, T., and Timasheff, S. N. (1996) *Protein. Sci.* 5, 372–381.
53. Wang, D., Bode, W., and Huber, R. (1985) *J. Mol. Biol.* 185, 595–624.
54. Tsukada, H., and Blow, D. M. (1985) *J. Mol. Biol.* 184, 703–711.
55. Wu, S. Y., Perez, M. D., Puyol, P., and Sawyer, L. (1999) *J. Biol. Chem.* 274, 170–174.
56. Diamond, R. (1974) *J. Mol. Biol.* 82, 371–391.
57. Howlin, B., Moss, D. S., and Harris, G. W. (1989) *Acta Crystallogr., Sect. A* 45, 851.
58. Smith, G. D., Duax, W. L., Dodson, E. J., Dodson, G. G., DeGraaf, R. A. G., and Reynolds, C. D. (1982) *Acta Crystallogr., Sect. B* 38, 3028.
59. Nogales, E., Wolf, S. G., and Downing, K. H. (1998) *Nature* 391, 199–203.
60. Martinez-Oyanedel, J., Choe, H.-W., Heinemann, U., and Saenger, W. (1991) *J. Mol. Biol.* 222, 335–352.
61. Berman, H. M., Westbrook, S., Feng, Z., Gilliland, G., Bhat, T. N., Weissig, H., Shindyalov, I. N., and Bourne, P. E. (2000) *Nucleic Acids Res.* 28, 235–242.
62. Miller, S., Janin, J., Lesk, A. M., and Chothia, C. (1987) *J. Mol. Biol.* 196, 641–656.
63. Gill, S. J., Dec, S. F., Olofsson, G., and Wadso, I. (1985) *J. Phys. Chem.* 89, 3758–3761.
64. Torres, A. M., Grieve, S. M., Chapman, B. E., and Kuchel, P. W. (1997) *Biophys. Chem.* 67, 187–198.
65. Brown, M. P., Grillo, A. O., Boyer, M., and Royer, C. A. (1999) *Protein Sci.* 8, 1276–1285.
66. Lundback, T., Hansson, H., Knapp, S., Ladenstein, R., and Hard, T. (1998) *J. Mol. Biol.* 276, 775–786.
67. Robinson, C. R., and Sligar, S. G. (1998) *Proc. Natl. Acad. Sci. U.S.A.* 95, 2186–2191.
68. Robinson, C. R., and Sligar, S. G. (1996) *Protein Sci.* 5, 2119–2124.
69. Sidorova, N. Y., and Rau, D. C. (1996) *Proc. Natl. Acad. Sci. U.S.A.* 93, 12272–12277.
70. Vossen, K. M., Wolz, R., Daugherty, M. A., and Fried, M. G. (1997) *Biochemistry* 36, 11640–11647.
71. Xavier, K. A., Shick, K. A., SmithGill, S. J., and Willson, R. C. (1997) *Biophys. J.* 73, 2116–2125.
72. von Hippel, P. H., and Schleich, T. (1969) Structure and Stability of Biological Macromolecules. In *Biological Macromolecules* (Timasheff, S. N., and Fasman, G., Eds.) Vol. 2, pp 417–573, Marcel Dekker, New York.
73. Ha, J.-H., Capp, M. W., Hohenwarter, M. D., Baskerville, M., and Record, M. T., Jr. (1992) *J. Mol. Biol.* 228, 252–264.
74. Overman, L. B., Bujalowski, W., and Lohman, T. M. (1988) *Biochemistry* 27, 456–471.
75. Garner, M. M., and Rau, D. C. (1995) *EMBO J.* 14, 1257–1263.
76. Kornblatt, J. A., et al. (1993) *Biophys. J.* 65, 1059–1065.
77. LiCata, V. J., and Allewell, N. M. (1998) *Biochim. Biophys. Acta* 1384, 306–314.
78. LiCata, V. J., and Allewell, N. M. (1997) *Biochemistry* 36, 10161–10167.
79. Reid, C., and Rand, R. P. (1997) *Biophys. J.* 72, 1022–1030.
80. Giorgione, J. R., and Epand, R. M. (1997) *Biochemistry* 36, 2250–2256.
81. Kornblatt, J. A., and Hoa, G. H. B. (1990) *Biochemistry* 29, 9370–9376.

BI992887L